Ontogeny of joint mechanics in squirrel monkeys (*Saimiri boliviensis*): functional implications for mammalian limb growth and locomotor development

Jesse W. Young

Department of Anthropology, University of Texas at Austin, Austin, TX 78712, USA

e-mail: jesse.young@mail.utexas.edu

SUMMARY

Juvenile animals must often compete against adults for common resources, keep pace during group travel and evade common predators, despite reduced body size and an immature musculoskeletal system. Previous morphometric studies of a diverse array of mammals, including jack rabbits, cats and capuchin monkeys, have identified growth-related changes in anatomy, such as negative allometry of limb muscle mechanical advantage, which should theoretically permit young mammals to overcome such ontogenetic limits on performance. However, it is important to evaluate the potential impact of such 'compensatory' growth trajectories within the context of developmental changes in locomotor behavior. I used standard kinematic and kinetic techniques to investigate the ontogenetic scaling of joint postures, substrate reaction forces, joint load arm lengths and external joint moments in an ontogenetic sample of squirrel monkeys (*Saimiri boliviensis*). Results indicated that young squirrel monkeys were frequently able to limit forelimb and hind limb joint loading *via* a combination of changes in limb posture and limb force distribution, potentially compensating for limited muscularity at younger ages. These results complement previous morphometric studies and suggest that immature mammals may utilize a combination of behavioral and anatomical mechanisms to mitigate ontogenetic limits on locomotor performance. However, ontogenetic changes in joint posture, not limb length *per se*, explained most of the variation in load arm lengths and joint loading in growing squirrel monkeys, indicating the importance of incorporating both anatomical and performance measures when studying the ontogeny of limb joint mechanics.

Supplementary material available online at http://jeb.biologists.org/cgi/content/full/212/025460/DC1

Key words: ontogenetic limitation, mechanical advantage, posture, kinetics, kinematics.

INTRODUCTION

Juvenile animals must often compete against adults for common resources, keep pace during group travel and evade common predators, despite ontogenetic limits on locomotor performance, such as reduced body size and an immature musculoskeletal system (Carrier, 1996). Because, by definition, juveniles have yet to reproduce, there should be strong selection for compensatory mechanisms, such as allometric musculoskeletal growth trajectories or developmental changes in behavior, that could enhance locomotor performance despite size- and growth-related limitations on performance (Pennycuick, 1975; Carrier, 1983; Werner and Gillam, 1984; Carrier and Leon, 1990; Irschick, 2000; Trillmich et al., 2003; Main and Biewener, 2004; Irschick et al., 2005; Young, 2005; Herrel and Gibb, 2006; Lawler, 2006). This study tests the hypothesis that allometric changes in joint mechanics allow growing squirrel monkeys to compensate for ontogenetic limits on locomotor performance.

At a given limb joint, the total muscular force necessary to counteract gravity is inversely proportional to the average distance of all muscle force vectors from the center of the joint (i.e. average of all muscle moment arms) and directly proportional to the product of the substrate reaction force (SRF) magnitude and its perpendicular distance from the joint (i.e. SRF load arm). This relationship can be represented as:

$$\mathbf{F}_\mathrm{M}r = \mathbf{F}_\mathrm{S}R , \qquad (1)$$

where $\mathbf{F}_\mathrm{M}$ is total muscle force, r is average muscle moment arm length (weighted by individual muscle force), $\mathbf{F}_\mathrm{S}$ is the magnitude

of the SRF and R is the SRF load arm (Gray, 1968; Biewener, 1983). Relative to whole body mass, newborn mammals typically have half as much muscle mass as adults (Grand, 1977; Goldspink, 1980; Grand, 1983; Atzeva et al., 2007; Bolter and Zihlman, 2007). Among squirrel monkeys, the species examined in this study, forelimb muscle mass as a percentage of body mass increases by 50% from neonates to adults and relative hind limb muscle mass more than doubles (Johnson, 1998). Young mammals therefore have relatively less available muscle force than adults, potentially compromising their ability to maintain joint postures during periods of intense limb loading, limiting performance capacity and potentially reducing fitness.

Carrier (Carrier, 1983) documented growth trajectories in black-tailed jackrabbits (*Lepus californicus*) and domestic cats (*Felis domesticus*) that theoretically permit these species to overcome ontogenetic limits on locomotor performance. In these animals, the length of the olecranon process at the elbow and the calcaneal tuberosity at the ankle, proportional to the average moment arms of m. triceps brachii and m. triceps surae, respectively, scale with negative allometry relative to the length of the anatomical segments distal to these joints (i.e. these muscles act on a relatively longer lever arm in younger animals). In a separate study of limb growth and locomotor development in domestic cats, Peters (Peters, 1983) corroborated Carrier's (Carrier, 1983) findings. Assuming that SRF load arms are proportional to limb length and SRF magnitudes are proportional to body weight, negative allometry of anatomical lever arms relative to limb length suggests that muscle mechanical advantage (i.e. r/R) should be greater in young animals, whereas

requisite muscle should be reduced, perhaps compensating for limited muscle mass and smaller body size. In a subsequent study, Carrier (Carrier, 1995) found that young jackrabbits were indeed able to achieve adult-like jumping velocities at only 30% of adult body size, thus confirming the link between allometric growth trajectories and enhanced locomotor performance at young ages. Carrier (Carrier, 1983) suggested that because identical scaling trends were found in distantly related jackrabbits and cats, negative allometry of muscle mechanical advantage might represent a generalized mammalian solution to ontogenetic limits on locomotor performance. In support of Carrier's (Carrier, 1983) hypothesis, Young (Young, 2005) recently documented a similar pattern of negative ontogenetic scaling of m. triceps brachii mechanical advantage in arboreal capuchin monkeys (*Cebus apella* and *Cebus albifrons*).

Carrier's (Carrier, 1983) and Young's (Young, 2005) analyses assumed that joint postures did not change during development and that SRF magnitudes remained a constant multiple of body weight. In other words, for the negative allometry of bony muscle lever arms to have the assumed effects, joint load arm lengths and joint moments should scale isometrically to body size. [For simplicity, external (i.e. SRF) joint moments will be referred to simply as joint moments throughout this paper. When referring to internal moments, the term muscle moment will be used.] If, however, developmental changes in joint postures and SRF magnitudes cause joint moments to scale allometrically, muscle lever growth trajectories may be more difficult to interpret. If joint moments are relatively greater in young animals, relatively longer bony muscle lever arms may not be sufficient to achieve adult-like levels of locomotor performance. Conversely, if joint moments are relatively smaller at early ages and increase over development, young mammals may not require relatively longer bony levers to increase performance.

This study focused on locomotor development in Bolivian (i.e. black-capped) squirrel monkeys [Platyrrhini: *Saimiri boliviensis* (Geoffroy and Blainville 1834)]. Squirrel monkeys are among the smallest anthropoid primates, with an average adult body mass of 811 g (Smith and Jungers, 1997). As a result, most squirrel monkey populations are under intense predation pressure (Fedigan et al., 1996). Predation risk has profoundly affected many aspects of squirrel monkey biology, including growth and development (Boinski, 1987; Boinski, 1999; Boinski et al., 2003). In a study of red squirrel monkey (*Saimiri oerstedi*) behavioral ecology in Costa Rica, Boinski (Boinski, 1987) found that infants experienced higher rates of predation than any other age class, with more than 50% of infants dying within the first six months of life. Similar rates of predation have been reported for *S. boliviensis* in Peru (Boinski et al., 2002). As a means of coping with predation risk early in life, squirrel monkey behavioral development is markedly precocial relative to that of other primates (Elias, 1977; Hartwig, 1995; Garber and Leigh, 1997). In captivity, infants engage in independent locomotion within the first month of life (Elias, 1977; Kaack et al., 1979; Fragaszy et al., 1991). In the wild, infants begin foraging independently within the first or second month of life, are traveling primarily independently by three months of age and are weaned between four and eight months of age (Boinski and Fragaszy, 1989; Mitchell, 1990; Stone, 2006). By six months of age, when juveniles are only 40–50% of adult size, foraging activity and locomotor repertoires are generally indistinguishable from adults (Boinski, 1989; Boinski and Fragaszy, 1989). Moreover, once juvenile squirrel monkeys have become independent, they must travel an average of 2–4 km day^{-1} to remain with the group and gain access to distributed foraging resources, such as fruit and invertebrate prey (Terborgh, 1983; Mitchell, 1990; Boinski, 1999).

In summary, squirrel monkeys are an excellent group in which to investigate how developmental changes in limb mechanics might impact locomotor performance in young mammals. In this study, I used standard kinematic and kinetic techniques to investigate the ontogenetic scaling of joint postures, SRF magnitudes and SRF joint moments in a longitudinal sample of growing Bolivian squirrel monkeys. Because squirrel monkeys use a variety of gaits across a diversity of substrates (Fontaine, 1990), I examined both symmetrical gaits (i.e. walking and running) and asymmetrical gaits (i.e. galloping and bounding) on terrestrial and simulated arboreal substrates (i.e. a flat runway and an 2.5 cm diameter elevated pole, respectively). Flat runway locomotion was sampled in order to remain consistent with previous studies of mammalian joint mechanics (e.g. Biewener, 1983; Schmitt, 1998; Polk, 2002; Witte et al., 2002) whereas locomotion on the pole was intended to represent a more naturalistic environment for arboreal squirrel monkeys. Additionally, in their natural environment, squirrel monkeys travel upon a variety of substrates that vary widely in diameter (Terborgh, 1983; Boinski, 1989; Fontaine, 1990; Mitchell, 1990). Sampling locomotion on the ground and a relatively narrow pole should represent the extremes of this variation in preferred substrate diameter. Because previous studies have assumed that limb growth is the primary determinant of ontogenetic variation in joint load arm lengths (e.g. Carrier, 1983; Young, 2005), I also measured limb segments (i.e. arm, forearm, thigh and leg lengths) at regular intervals and used path analysis (Li, 1975) and hierarchical partitioning (Chevan and Sutherland, 1991) to investigate the independent influence of limb length and posture on developmental changes in joint load arm lengths.

I tested two null hypotheses, based on the morphometric findings of Carrier (Carrier, 1983) and Young (Young, 2005). First, when growing squirrel monkeys are traveling at the same absolute speed, joint angles, SRF magnitudes, SRF angles, joint load arm lengths and joint moments should scale isometrically to body size. Specifically, angular variables should remain constant throughout ontogeny, SRF magnitudes should scale to body weight, joint load arm lengths should scale to the cube root of body mass, and joint moments should scale to body mass. Second, I predicted that ontogenetic variation in joint load arm lengths should be primarily determined by ontogenetic variation in limb length distal to the joint in question. To examine the independent and overall influence of limb length on joint load arm length, I constructed path models (Li, 1975) specifying the hypothesized influence of limb length, joint posture, limb posture and SRF orientation on joint load arm length. The general organization and predicted form of the path models are presented in Fig. 1.

MATERIALS AND METHODS
Animal subjects

Five female infant–juvenile squirrel monkeys constituted the sample for this study. An additional squirrel monkey participated in two experiments but had to be withdrawn because of an unrelated tail injury. Collectively, the squirrel monkeys ranged in age from 74 to 302 days, and in body mass from 218 to 535 g (29–71% of adult size; mean: 367 g). Participation duration for individual monkeys ranged from 151 to 185 days (mean: 172.2 days; median: 179 days), beginning at ages of 74–120 days (mean: 104.6 days; median: 118 days). The age range sampled in
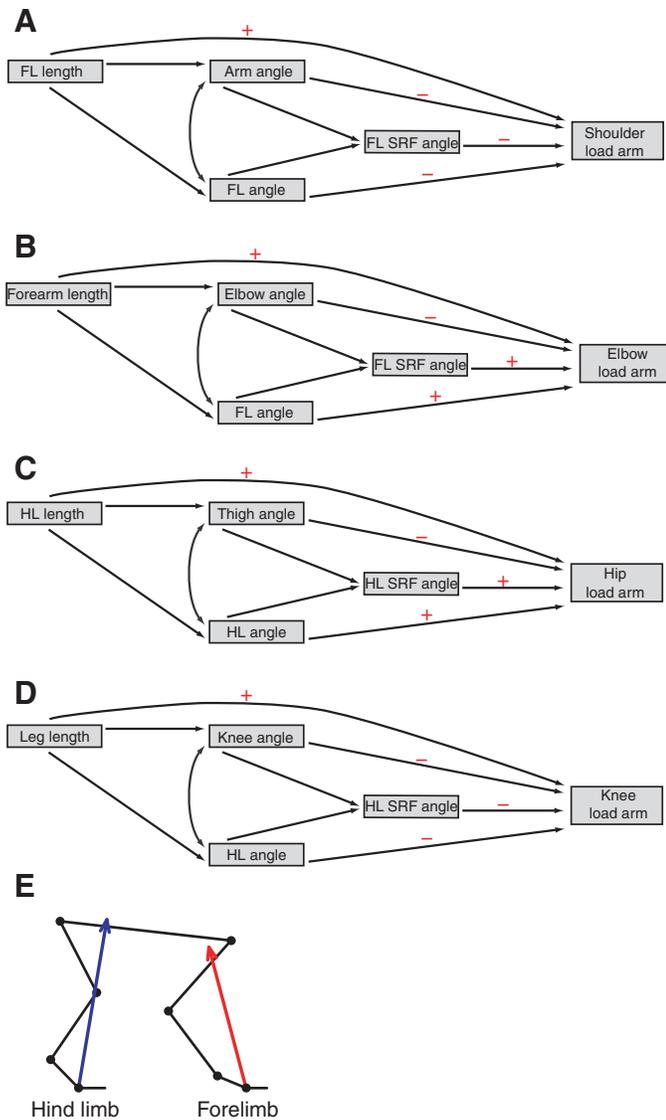
Fig. 1. Path diagrams specifying the hypothesized influence of limb length, joint posture, limb posture and substrate reaction force (SRF) orientation on joint load arm length. (A) Shoulder, (B) elbow, (C) hip and (D) knee joints. (E) A schematic representation of average forelimb and hind limb postures across the current dataset to help visualize the predicted effects of variation in posture and SRF orientation on load arm lengths. Red and blue lines indicate the average orientation of forelimb and hind limb SRF, respectively. Within the path diagrams, single-headed arrows indicate a directed causal link between predictor variables and moment arm lengths. Double-headed arrows indicate an undirected correlation between predictor variables. Red + and – symbols indicate the predicted direction of the relationship. For all joints, limb length was predicted to have a positive effect on load arm length. Because joint extension is a well-established means of shortening joint load arms (Gray, 1968; Biewener, 1989), larger, more extended, joint angles were predicted to decrease joint load arm lengths. The influence of limb angles was predicted to vary according to limb and joint (cf. E). Increasing forelimb protraction and hind limb retraction while maintaining SRF orientation should bring the limb axis more in line with the SRF vector, thus shortening shoulder/hip load arms but increasing the distance between the middle joint and the SRF vector and lengthening elbow/knee load arms. Similarly, cranial deviation of forelimb SRF angles should decrease shoulder load arm lengths and increase elbow load arm lengths, whereas caudal deviation of hind limb SRF angles should increase hip load arm lengths but increase knee load arm lengths.

this study (i.e. 74–302 days) therefore encompasses the period during which wild squirrel monkeys begin locomoting independently, gain foraging competence and become independent juveniles. Monkeys lived in social groups of 15–30 individuals that were housed in large $1.5\,m \times 2.1\,m \times 4.5\,m$ enclosures with 35–40 linear meters of perches and substrates for free-ranging locomotor activity. Research was performed at the Center for Neotropical Primate Research and Resources (CNPRR: Mobile, AL, USA). Institutional Animal Care and Use Committees (IACUC) at Stony Brook University and the CNPRR approved all procedures before the start of this research.

Data collection

Before each experiment, individuals were weighed and the skin over the approximate centers of rotation of the shoulder, elbow, wrist, hip, knee and ankle were shaved and marked with retro-reflective tape (3M Corporation, St Paul, MN, USA), a procedure that did not require the use of anesthetic. Anatomical landmarks used to identify approximate joint centers of rotation are listed in Table 1. Arm, forearm, thigh and leg lengths, measured as the distance between adjacent landmarks, were also recorded at this time. Monkeys were then filmed as they traversed a 2.75 m enclosed linear runway using a high-speed digital video camera (MotionMeter 1000, Redlake MASD, San Diego, CA, USA) operating at 250 Hz. Depending on experimental condition (e.g. ground or pole), monkeys traversed either the flat runway floor or a 2.5 cm diameter PVC pipe elevated 10.7 cm above the surface of the runway. Speed was not controlled during locomotion. Rather, at all ages, animals were permitted to self-select preferred speeds.

Two custom-built $30.5\,cm \times 30.5\,cm$ triaxial force platforms (Heglund, 1981; Biewener and Full, 1992), placed in series in the center of the runway, were used to measure locomotor kinetics. During the simulated arboreal trials, PVC segments (30.5 cm long and 2.5 cm in diameter) were attached to each force platform by bolts secured directly to the platform frame. Voltage outputs from channels corresponding to each force axis were routed through a National Instruments (Austin, TX, USA) SC-2345 chassis and recorded using a LabView virtual instrument. Cross talk between force channels was generally low, ranging between 0.3% and 3.5% without the pole segment and 0.3% and 10.5% when the pole segment was attached. Force platforms were calibrated daily following the recommendations of Biewener and Full (Biewener and Full, 1992).

Following the method of Riskin et al. (Riskin et al., 2005), kinetic and kinematic data were synchronized using a 3.3 V square-wave pulse generated by the video camera and routed separately to a bank of LEDs positioned on the back wall of the runway and to the SC-2345 chassis. This circuit was normally interrupted by means of a handheld switch. During each trial, the switch was briefly closed, simultaneously illuminating the LEDs and changing the shape of the square wave in the data file. Using this procedure, it was possible to synchronize video and kinetic data to a resolution of four milliseconds.

Video files from each experiment were imported into the MATLAB DLT Dataviewer 2 digitizing platform (Hedrick, 2007) for coding on a trial by trial basis. Individual strides were identified based on the cyclic touchdowns of a reference limb. For steps (i.e. stance phases) in which single-limb kinetic data were available, the two dimensional position of all limb landmarks and the fifth metapodial head were digitized at peak vertical force. Owing to the small size of the young monkeys, reflective markers could not be attached to the skin overlying the metacarpal and metatarsal heads.

Table 1. Anatomical landmarks used to approximate joint centers of rotation

Joint	Anatomical landmark
Shoulder	Midpoint between the acromion process of the scapula and the greater tubercle of the humerus
Elbow	Midpoint between the lateral epicondyle of the humerus and the lateral aspect of the radial head
Wrist	Radial styloid process
Hip	Greater trochanter of the femur
Knee	Midpoint between the lateral epicondyle of the femur and the lateral condyle of the tibia
Ankle	Lateral malleolus of the fibula

Therefore, the position of these landmarks was estimated to be at the base of the fifth manual/pedal ray.

Force data from each trial were imported into MATLAB (Mathworks, Natick, MA, USA), transformed into Newtons and corrected for cross talk. Force traces from each channel were smoothed using a zero-lag fourth-order Butterworth low-pass filter with a cut-off frequency of 25 Hz. Baseline drift during and between trials was corrected by sampling the average values of unloaded periods immediately before and following platform contact and subtracting these values from the force traces. Overall, baseline drift was extremely low, averaging less than $3\,\mathrm{mN\,s^{-1}}$ across force channels and substrate conditions (ground: vertical=$2.7\pm2.84\,\mathrm{mN\,s^{-1}}$, fore–aft=$2.4\pm6.10\,\mathrm{mN\,s^{-1}}$; mediolateral=$1.1\pm0.97\,\mathrm{mN\,s^{-1}}$; pole: vertical=$2.0\pm1.52\,\mathrm{mN\,s^{-1}}$, fore–aft=$1.1\pm1.28\,\mathrm{mN\,s^{-1}}$; mediolateral=$0.9\pm1.80\,\mathrm{mN\,s^{-1}}$). On average, these values equated to less than 0.3% of the maximum force recorded during a given trial. Because step durations averaged $0.13\pm0.066\,\mathrm{s}$ across the dataset, the maximum average amount of drift during a single contact period with the force plates would have been 0.35 mN. Baseline drift thus exerted a negligible effect on force platform accuracy and precision.

Single-limb contacts were recognized when a forelimb or hind limb contacted the force platform in isolation and ended when the limb either left the platform or another limb touched down. Because the monkeys frequently placed limbs in close proximity during locomotion, obtaining isolated single-limb contacts was often difficult. Trials with overlapping limb contacts on a single force platform were retained only when peak vertical force was clearly identifiable and the vertical force trace had returned to 50% of the peak value prior to rising again in the case of forelimb contacts, or began its rise at no more than 50% of the former vertical force peak in the case of hind limb contacts. An exemplar stride illustrating the experimental apparatus used for kinematic and kinetic data collection is shown in supplementary movie 1 (see supplementary movie).

Dependent variables
Speed
Average locomotor speed was calculated from the sagittal displacement of either the shoulder or the hip, depending on marker visibility. Examination of trials in which both hip and shoulder data were available revealed that hip and shoulder speed varied on average by $0.02\pm0.054\,\mathrm{m\,s^{-1}}$, or approximately 1.1% of average forward speed. Digitizing noise was corrected using a zero-lag fourth-order Butterworth low-pass filter with a cut-off frequency of 10 Hz. This cutoff frequency was selected as optimal using a residual analysis procedure described by Winter (Winter, 2005). Piecewise cubic spline interpolation was used to interpolate over gaps of missing data ≤10 frames (i.e. 40 ms). After transforming raw pixel coordinates into meters by using the force platforms as calibration objects, linear least-squares regressions of corrected displacement data on time were used to calculate overall speed across each stride.

Trials in which the coefficient of determination (i.e. R^2) of reference marker position against time was less than 0.99 were designated unsteady and discarded.

Gait
To distinguish between symmetrical and asymmetrical strides, stride symmetry was calculated as the absolute duration between the touchdowns of contralateral forelimb and hind limb pairs (e.g. right and left forelimbs) expressed as a percentage of total stride duration. Following Hildebrand (Hildebrand, 1976), strides in which both forelimb and hind limb symmetry was between 43.75% and 56.25% were designated symmetrical; all other strides were designated asymmetrical. Data from leading and trailing limbs within asymmetrical gaits were treated separately for allometric analyses of joint mechanics.

Joint kinematics
Segment angles (i.e. forelimb, arm, hind limb and thigh angles) were calculated as the two-dimensional vector angle between the relevant limb segment and the vertical axis. Forelimb and hind limb segments were defined by a line joining the shoulder or hip to the metapodial head. Joint angles (e.g. elbow or knee angle) were calculated as the two-dimensional vector angle between the relevant limbs segments (e.g. arm and forearm or thigh and leg).

Kinetic variables
The angle of the SRF with respect to the vertical axis was calculated as:

$$\tan^{-1}\left(\frac{\mathbf{F}_{x(Vpk)}}{\mathbf{F}_{y(Vpk)}}\right), \qquad (2)$$

where $\mathbf{F}_{x(Vpk)}$ and $\mathbf{F}_{y(Vpk)}$ are, respectively, the magnitudes of the fore–aft and vertical components of the SRF at peak vertical force. Negative values indicate that the SRF was caudally inclined, whereas positive angles indicate that the SRF was cranially inclined. The resultant magnitude of the sagittal component of the SRF was calculated as:

$$\sqrt{\mathbf{F}_{x(Vpk)}^2 + \mathbf{F}_{y(Vpk)}^2}. \qquad (3)$$

Because only sagittal (i.e. two-dimensional) kinematic data were recorded, the mediolateral component of SRF was not included in the above calculations. However, peak mediolateral force magnitudes were consistently minor (i.e. approximately 5% of peak vertical force magnitudes) and therefore had little effect on the magnitude or resultant orientation of the SRF. Following previous studies of mammalian joint mechanics (e.g. Biewener, 1983; Schmitt, 1998; Polk, 2002; Witte et al., 2002), SRFs were assumed to pass through the metapodial heads at the moment of peak vertical SRF. Joint moments were calculated as the cross (i.e. vector) product of the SRF and the two-dimensional position vector connecting the metacarpal/metatarsal head to the joint in

question (Ozkaya and Nordin, 1999). Load arm lengths were computed by dividing joint moments by the SRF magnitude (Polk, 2001). Positive values signify flexing moments arms (dorsiflexing at the wrist and ankle), whereas negative values signify extending moments (palmar- and plantarflexing at the wrist and ankle).

It should be noted that the methods used here did not account for the effects of limb segment inertia or gravity on calculated joint moments. However, the present analysis was explicitly concerned with the effects of ontogenetic variation in limb posture and SRF on joint mechanics. The effects of ontogenetic changes in limb inertial properties is a related, but separate, issue that should certainly be examined in additional studies (e.g. Raichlen, 2006). Moreover, in the small-bodied quadrupeds examined here, inertial forces are likely to be minor relative to SRF (Biewener and Full, 1992). Indeed, Witte et al. (Witte et al., 2002) have recently shown that inertial forces account for no more than 10% of total limb joint moments among small quadrupedal mammals (i.e. 150–400 g in body mass).

To adjust for ontogenetic differences in body size, SRF magnitudes were divided by body weight, load arm lengths were divided by the cube root of body mass and joint moments were divided by body mass, following Witte et al. (Witte et al., 2002). Scaling joint moments to body mass follows from the isometric expectation that muscle lever arm lengths, as linear dimensions, scale to the cube root of body mass (i.e. $\propto M_b^{0.33}$), whereas muscle force, proportional to physiological cross-sectional area, scales to the two-thirds power of body mass (i.e. $\propto M_b^{0.67}$). Muscle moments, equal to the product of force and length, should therefore scale directly to body mass (i.e. $M_b^{0.33} \times M_b^{0.67}$). Mass-adjusted joint moments therefore provide a metric of load magnitude relative to theoretically available muscle moments. This scaling procedure necessarily assumes that muscle moments scale isometrically to body mass in growing squirrel monkeys, a proposition that remains to be tested. Nevertheless, this assumption is consistent with previous morphometric studies of developmental joint mechanics (i.e. Carrier, 1996; Young, 2005), where it is argued that increased muscle mechanical advantage would be required to compensate for reduced muscularity at young ages and isometrically maintain similar mass-adjusted muscle moments throughout ontogeny.

Statistical analyses

To increase statistical power, data from individual monkeys were combined to create mixed longitudinal samples for all analyses. Body mass, which was strongly positively correlated with age across individuals (Fig. 2), was used as the primary independent variable in all ontogenetic analyses. Moreover, because of the precocial nature of squirrel monkey behavioral development (Elias, 1977; Hartwig, 1995), size should have a stronger effect on locomotor mechanics than age *per se* (cf. Schilling, 2005).

Morphometric data were tested for allometric growth by fitting log-transformed segment lengths and body masses to the standard allometric power function (Huxley, 1932) using Model II reduced major axis (RMA) regression (Ricker, 1984). Confidence intervals on RMA slopes were calculated following Pitman (Pitman, 1939). Allometry was identified when the 95% confidence intervals for the calculated slopes did not include 0.333. Regressions were performed using the (S)MATR software package (Falster et al., 2003).

To characterize intra-limb variability in joint loading across the ontogenetic sample, forelimb and hind limb joint moments were specified as within-subjects factors in repeated-measures analyses of variance (ANOVA). In cases where limb joint moments varied
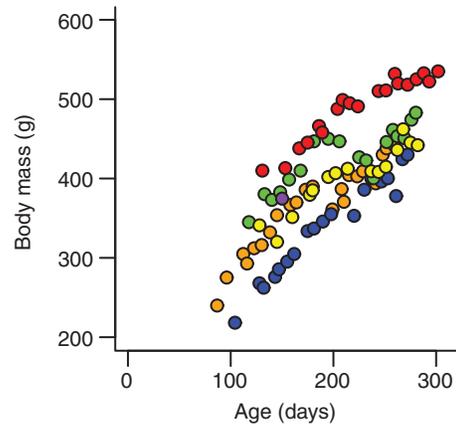

Fig. 2. Body mass plotted against age for all infant *Saimiri boliviensis*. Body mass was strongly positively correlated with age in each infant. Red circles, animal 4428 (r=0.957); purple circles, animal 4433; yellow circles, animal 4445 (r=0.938); green circles, animal 4466 (r=0.855); blue circles, animal 4475 (r=0.977); orange circles, animal 4483 (r=0.947). A correlation coefficient was not computed for animal 4433 because of this animal's limited participation in the study.

as a linear function of body mass and/or speed, repeated-measures analyses of covariance (ANCOVA) were used *in lieu* of ANOVA, specifying mass and/or speed as the covariate(s). Paired *t*-tests between group means (least-squares adjusted means following ANCOVA) were used to test for significant *post-hoc* differences between joints. Analyses were performed separately by substrate, gait type and limb order (in the case of asymmetrical gaits) using SPSS 11.0.4 (SPSS, Chicago, IL, USA).

Partial correlations were used to investigate the influence of body mass on each variable while controlling for speed. The null hypothesis for each test was that body mass had no association with the dependent variable. Because all variables were either dimensionless (i.e. angles) or were adjusted for body size differences prior to analysis, any significant correlation indicated allometry (Mosimann and James, 1979). Correlation analyses were again performed separately by gait type, substrate and limb order (in the case of asymmetrical strides) using SPSS 11.0.4.

Hierarchical partitioning (Chevan and Sutherland, 1991) and path analysis (Li, 1975; Sokal and Rohlf, 1995) were used to dissect the independent influence of limb length and posture on observed variation in absolute joint load arm lengths. Both hierarchical partitioning and path analysis can be thought of as extensions of multiple regression. Given a linear model with one dependent variable (Y) and k independent variables (X_1, X_2, X_3…X_k), hierarchical partitioning quantifies the independent contribution of each X variable to the total coefficient of determination for Y as the average change in R^2 produced by adding the variable to a hierarchical series of increasingly complex models. The significance of each variable's independent contribution to the total coefficient of determination can be tested using a randomization procedure introduced by MacNally (MacNally, 2002). Hierarchical partitioning was performed using the hier.part package (MacNally and Walsh, 2004) of the R statistical platform (R Development Core Team, 2008).

Path analysis (Li, 1975; Sokal and Rohlf, 1995) was used to clarify the independent and associative influence of limb lengths on load arm lengths. In a path analysis, each hypothesized causal link (i.e. direct association) between variables is represented

diagrammatically by a single-headed arrow and is associated with a path coefficient – equivalent to a standardized partial regression coefficient in a multiple regression. Additionally, predictor variables can be joined *via* undirected double-headed arrows (equivalent to a standard bivariate correlation), signifying that the variables are related to one another without specifying a necessary causal structure. Once a path diagram has been constructed, and all associated path coefficients have been specified, the 'indirect' association between any predictor and a criterion variable can be quantified as the summation of all the products of coefficients linking the two variables (Sokal and Rohlf, 1995).

Path models were fit to the data using iterative maximum likelihood estimation (Schermelleh-Engel et al., 2003). Each path model was initially fit with all of the hypothesized paths included in the model. Non-significant paths were then removed from model specification and the model was refit, resulting in the most parsimonious model for the data. The overall fit of each path model was evaluated by calculating χ^2 tests that compared the empirically observed correlation matrix to the correlation matrix implied by the model. Non-significant χ^2 tests (i.e. *P*>0.05) indicate a good fit between the model and the data (Schermelleh-Engel et al., 2003). All path analyses and associated tests of fit were performed using the AMOS 16 software package (AMOS Development Corporation, Spring House, PA, USA). Only trials without missing data for any of the parameters were included in the path analyses.

Because the goal of hierarchical partitioning and path analyses was to test the hypothesis that joint load arms were directly proportional to anatomical limb length distal to the joint in question, only those joints for which the relevant limb lengths were available (i.e. shoulder, elbow, hip and knee joints) were included in these analyses. Additionally, because path analysis requires large sample sizes to obtain effective power (typically ≥10 times the number of parameters included in the model) (Schermelleh-Engel et al., 2003), data were pooled across gaits within substrates. Previous analyses of this data set indicated that the path models were statistically similar across gait types within substrates. Specifically, significant differences between path coefficients from symmetrical *versus* asymmetrical path models within substrates were found in only three out of 72 possible cases (i.e. nine parameters per path model × four joints × two substrates).

RESULTS

A total of 664 strides were analyzed. The tabulation of strides and forelimb and hind limb steps by substrate, gait type and limb order (for asymmetrical strides) is shown in Table 2.

Table 2. Number of strides and forelimb and hind limb steps in the data set, grouped by substrate, gait type and limb order for asymmetrical gaits

	Ground	Pole
Symmetrical gaits		
Total strides	84	155
Forelimb steps	61	114
Hind limb steps	44	95
Asymmetrical gaits		
Total strides	187	238
Leading limbs		
Forelimb steps	26	95
Hind limb steps	33	46
Trailing limbs		
Forelimb steps	123	105
Hind limb steps	34	76

Ontogenetic scaling of limb length

In the sample of squirrel monkeys measured here, all segment lengths scaled to body mass with strong positive allometry (Fig. 3), indicating that smaller and younger monkeys were relatively short-limbed for their body size. Forelimb segments tended to scale with greater positive allometry than hind limb segments, although only the forearm scaled significantly faster than hind limb segments (*P*≤0.01 for all comparisons). Scaling exponents describing overall forelimb and hind limb growth indicated strong positive allometry for both limbs. Total forelimb length scaled with significantly greater positive allometry than total hind limb length (*P*<0.05).

Ontogenetic scaling of joint mechanics

Across the ontogenetic sample, most forelimb and hind limb joints primarily experienced flexing (i.e. positive) joint moments at peak vertical force (Fig. 4), regardless of gait type or substrate. The only consistent exception was the knee joint, which experienced a combination of weakly flexing and extending moments. The hip and shoulder joints also occasionally experienced extending moments, particularly during asymmetrical gaits. Forelimb joint moment magnitudes were consistently greatest at the elbow, regardless of substrate, gait or limb order (all *P*<0.001). Wrist moments were significantly greater than shoulder moments during all locomotion on the ground (all *P*<0.05), whereas shoulder and wrist moments were statistically similar during locomotion on the pole. Hind limb joint moment magnitudes were consistently smallest at the knee (all *P*<0.05). Hip moments were significantly greater than ankle moments during symmetrical gaits (all *P*<0.001), regardless of substrate, and for leading limbs during asymmetrical gaits on the ground (*P*<0.01). In all other conditions, hip and ankle moments were statistically similar.

Absolute locomotor speed and body mass were significantly positively correlated during asymmetrical gaits on the pole, but were unrelated during all other substrate-by-gait conditions (Table 3). Relative speed [i.e. Froude number: $u(gh)^{-0.5}$, where *u* is speed, *g* is gravitational acceleration (9.81 m s^{-2}) and *h* is the average of hip and shoulder heights at peak vertical force] (Biewener, 2003) also changed little with speed (Table 3). As with absolute speed, relative speed was significantly positively correlated with body mass during asymmetrical gaits on the pole, but was unrelated to body mass during all other conditions. Overall, these data indicate that squirrel monkeys used a wide variety of speeds across the ontogenetic series and that the youngest monkeys frequently moved as fast as older and larger monkeys.

Partial correlations describing the independent association between body mass and all other kinematic/kinetic parameters, controlling for absolute speed, are shown in Table 3. Previous analyses of this dataset (Young, 2008a) indicated that the patterns shown in Table 3 remained consistent when partial correlations were calculated controlling for relative, rather than absolute, speed. Specifically, out of the 144 correlations displayed in Table 3 (i.e. 24 parameters × six substrate-by-gait conditions), significant differences between absolute speed-adjusted and relative speed-adjusted correlations were only found in seven cases.

Joint kinematics

Forelimb angle changed minimally with body mass, becoming significantly more protracted during symmetrical gaits on the ground and for leading limbs during asymmetrical gaits on the pole, but showing no other significant changes as body size increased. By contrast, elbow angle became significantly more flexed with increasing mass in all conditions except for symmetrical gaits on
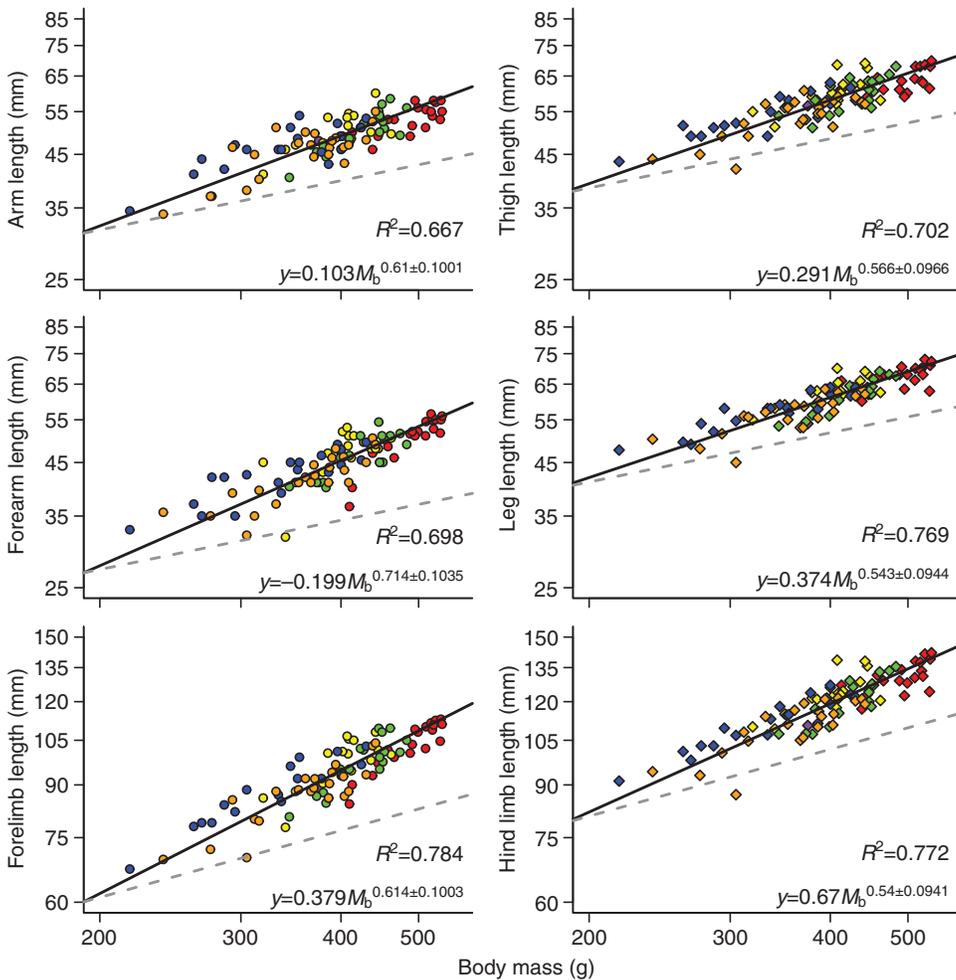
Fig. 3. Allometry of limb growth in *Saimiri boliviensis*. Data are plotted on log–log axes. Black lines indicate the calculated reduced major axis (RMA) slopes for each segment computed across individuals. Dashed gray lines indicate isometry. Forelimbs and forelimb segments are represented by circles whereas hind limbs and hind limb segments are represented by diamonds. Color codes for individual monkeys follow Fig. 1. Graphs are plotted on the same scale to indicate absolute differences in segment length. Allometric regression equations and coefficients of determination (i.e. R^2 values) are provided for each relationship at the bottom of the plot.

the ground and for leading limbs during asymmetrical gaits on the ground. Changes in arm angle principally tracked changes in elbow angle, becoming significantly more retracted during symmetrical gaits on the pole and for trailing limbs during asymmetrical gaits on the pole. Wrist angle did not change with size during symmetrical gaits, but became significantly more flexed for leading limbs during asymmetrical gaits on the ground and significantly more extended in all other asymmetrical gait conditions.

As with forelimb angle, hind limb angle changed little with increasing body mass, becoming significantly more protracted during symmetrical gaits on the ground and for leading limbs during asymmetrical gaits on the pole, but remaining static in all other conditions. Knee angle became significantly more flexed during symmetrical gaits on the pole but did not significantly change in any other condition. Size-related changes in thigh angle tracked changes in knee and hind limb angles, becoming significantly more flexed (i.e. protracted) during symmetrical gaits on the pole and for leading limbs during asymmetrical gaits on the pole. Ankle angle did not significantly vary with body size in any condition.

Force vectors

Relative forelimb force magnitudes significantly decreased with increasing body size across all conditions except for leading limbs during asymmetrical gaits on the ground. By contrast, relative hind limb peak force magnitudes significantly increased during symmetrical gaits on both substrates and for leading limbs during asymmetrical gaits on the pole, and showed non-significant trends

to increase in all other conditions except for trailing limbs during asymmetrical gaits on the pole. Forelimb force angles significantly decreased with size (i.e. became significantly more caudally oriented) during symmetrical gaits on the ground and for leading limbs during asymmetrical gaits on the pole. Similarly, hind limb force angles significantly decreased for leading limbs during asymmetrical gaits on the pole. In each of these cases, caudal reorientation of the SRF vector corresponded to significant increases in limb protraction with increasing size. Similarly, forelimb force angles for leading limbs during asymmetrical gaits on the ground became significantly more cranially oriented as size increased, corresponding to a nearly significant increase in forelimb retraction ($P=0.066$). Altogether, these results suggest that both the fore- and hind limbs were operating at least partly as struts (i.e. the SRF vector was oriented along the effective axis of the limb) (Barclay, 1953; Gray, 1968).

Joint load arm lengths

Variation in relative joint load arm lengths principally tracked variation in joint angles. Increases in elbow flexion corresponded to significant size-related increases in relative elbow load arm lengths during symmetrical gaits on the pole, for leading limbs during asymmetrical gaits on the pole, and for trailing limbs during asymmetrical gaits on both substrates. Similarly, increases in wrist extension corresponded to decreases in relative wrist load arm lengths during asymmetrical gaits on the pole, regardless of limb order. Among the hind limb joints, significant changes were only
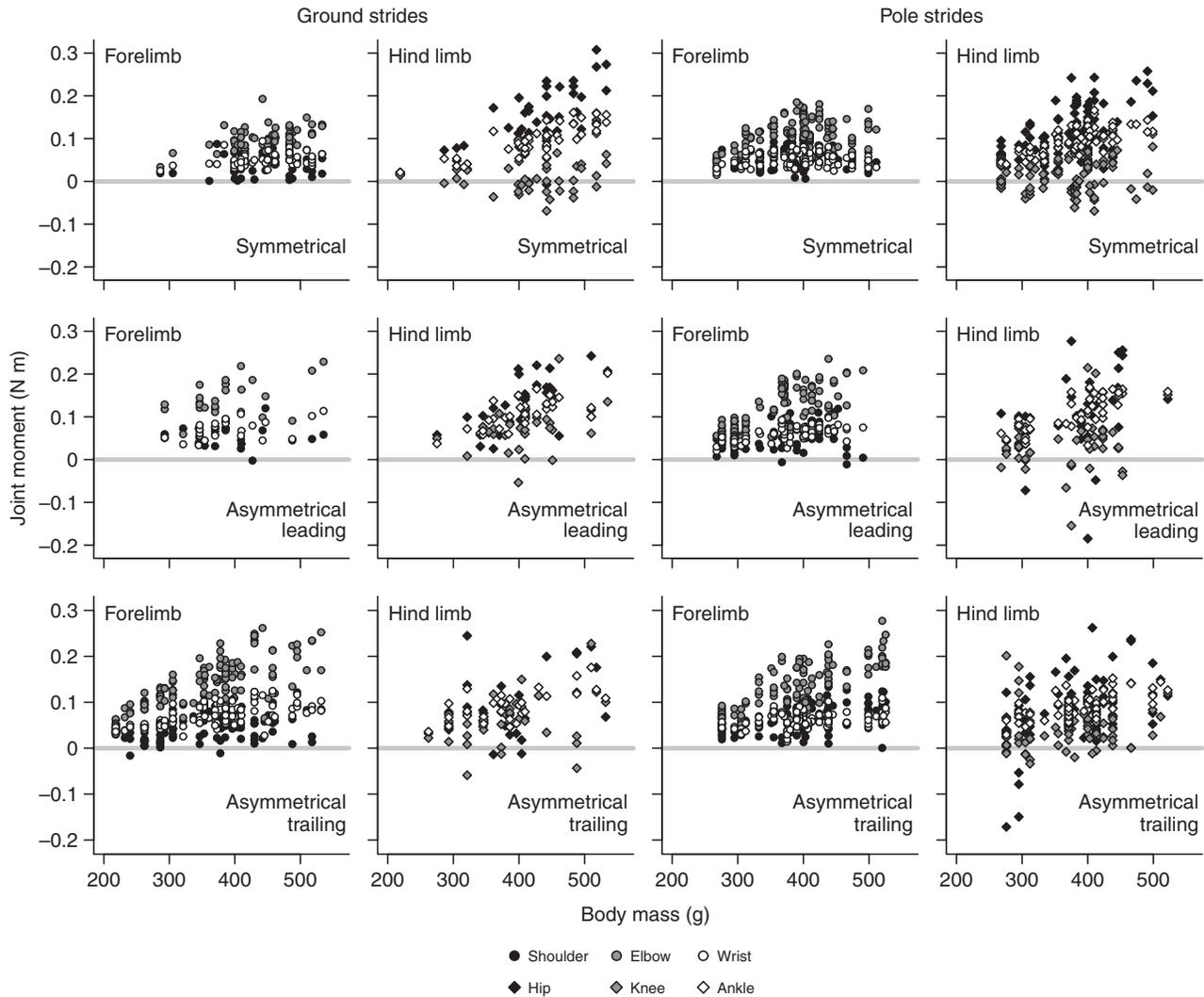
Fig. 4. Scatter plots of absolute joint moment magnitudes *versus* body mass in all substrate and gait conditions. The gray horizontal bar indicates the division between positive flexing moments and negative extending moments.

observed during symmetrical gaits on the ground, where hip and ankle load arms became longer with increasing body size. By contrast, knee load arms decreased during symmetrical gaits on the ground, in fact passing from the flexing to the extending side of the joint (Fig. 4).

Joint moments

Significant size-related increases in relative moments were observed at several joints in multiple conditions. In the forelimb, relative elbow moments increased during symmetrical gaits on the pole, in leading forelimbs during asymmetrical gaits on the pole, and in trailing forelimbs during asymmetrical gaits on both substrates. In the hind limb, relative hip and ankle moments increased during all conditions except for trailing limbs during asymmetrical gaits on the ground. Size-related increases in relative knee moments were observed for trailing limbs during asymmetrical gaits on the ground. The only significant size-related decrease in relative moments was at the wrist joint for trailing limbs during asymmetrical gaits on the pole. Relative moments at all other joints and conditions remained static with increasing body size.

Effects of limb length and posture on joint load arm lengths

The results of hierarchical partitioning and path analyses of the influence of limb length and posture on shoulder, elbow, hip and knee load arm lengths are presented graphically in Fig. 5 for strides on the ground and Fig. 6 for strides on the pole. The direct, indirect and total effects of limb lengths on load arm lengths, as implied by the path models, are shown in Table 4. Overall, the path models described here predicted patterns of correlation among limb lengths, joint postures, limb postures, SRF angles and load arm lengths very well, as indicated by non-significant χ^2 statistics in all cases (all $P \geq 0.23$).

Shoulder load arm lengths

Variation in forelimb length, arm angle, forelimb angle and forelimb SRF angle collectively explained 97.6–97.8% of the variance in shoulder load arm lengths across the ontogenetic sample. Forelimb angle and SRF angle were consistently the best predictors of shoulder load arm length, irrespective of substrate. Together, these two variables explained more than 90% of the variation in shoulder load arm length on both substrates. Forelimb and SRF angles were negatively correlated, as expected if the limbs were at least partly

Table 3. Correlations between kinematic/kinetic parameters and body mass

	Symmetrical gaits		Asymmetrical gaits: leading limbs		Asymmetrical gaits: trailing limbs	
	Ground	Pole	Ground	Pole	Ground	Pole
Speed	0.152	0.015	–0.020	**0.567**	–0.019	**0.318**
Froude number	0.071	–0.027	–0.162	**0.382**	–0.164	**0.238**
Joint kinematic*s*						
Forelimb	**0.289**	0.141	–0.374	**0.275**	0.051	–0.136
Arm	0.205	**–0.213**	–0.397	–0.101	–0.021	**–0.578**
Elbow	–0.038	**–0.418**	–0.002	**–0.446**	**–0.298**	**–0.638**
Wrist	0.076	0.145	**–0.462**	**0.434**	**0.303**	**0.305**
Hindlimb	**0.493**	0.189	0.047	**0.466**	0.135	0.218
Thigh	0.225	**0.286**	0.105	**0.489**	0.167	0.204
Knee	0.118	**–0.211**	–0.235	–0.054	–0.120	–0.061
Ankle	0.201	–0.192	–0.077	0.127	0.077	–0.051
Force vectors						
FL magnitude	**–0.411**	**–0.495**	**–0.449**	0.024	**–0.402**	**–0.454**
FL angle	**–0.328**	–0.032	**0.621**	**–0.221**	–0.141	0.107
HL magnitude	**0.754**	**0.250**	0.285	**0.310**	0.214	–0.075
HL angle	–0.178	–0.134	0.094	**–0.427**	–0.205	–0.055
Joint load arms						
Shoulder	–0.059	–0.115	–0.244	–0.176	0.079	0.058
Elbow	0.128	**0.367**	0.203	**0.319**	**0.194**	**0.470**
Wrist	–0.085	–0.105	–0.305	**–0.221**	–0.049	**–0.227**
Hip	**0.505**	0.154	0.326	0.236	–0.020	0.226
Knee	**–0.329**	0.045	0.030	–0.177	0.227	–0.169
Ankle	**0.295**	0.144	0.246	0.115	–0.119	0.171
Joint moments						
Shoulder	–0.102	–0.172	–0.335	–0.046	0.125	0.061
Elbow	0.016	**0.205**	–0.028	**0.404**	**0.300**	**0.318**
Wrist	–0.099	–0.178	0.049	0.045	0.111	**–0.262**
Hip	**0.673**	**0.329**	**0.428**	**0.312**	0.181	**0.275**
Knee	–0.085	0.053	0.198	–0.103	**0.467**	–0.150
Ankle	**0.730**	**0.452**	**0.439**	**0.415**	0.286	**0.295**

Bivariate correlations are shown for speed/Froude number *versus* body mass. All other correlations are partial correlations between the indicated parameter and body mass, controlling for speed. Bold print indicates significance ($P<0.05$).

FL, forelimb; HL, hind limb.

operating as struts (Barclay, 1953; Gray, 1968). Increases in forelimb angle (i.e. greater protraction), were associated with shorter shoulder joint load arms, even when controlling for SRF orientation, supporting the prediction that a more protracted forelimb places the shoulder joint more in line with the caudally inclined SRF vector, thereby mitigating load arms and moments.

Forelimb length explained just 2.2–3.6% of the variance in shoulder load arm length. Across substrates, most of the total correlation between forelimb length and shoulder load arm length was due to the direct effect of forelimb length (Table 4). Negative indirect correlations between forelimb length and shoulder load arm length, operating *via* arm and forelimb angle, slightly mitigated the total correlation between forelimb length and shoulder load arm lengths on both substrates. In sum, longer forelimbs were weakly associated with increases in shoulder joint load arms lengths, and this relationship was made even weaker when the effects of limb length on joint posture were included in the model.

Elbow load arm lengths

Variation in forearm lengths, elbow angles, forelimb angles and forelimb SRF angles explained 85.7–87.5% of the variance in elbow load arm lengths. As predicted (Fig. 1), increases in forearm length, elbow flexion, forelimb protraction and forelimb SRF angle were all associated with longer elbow load arms. Across substrates, elbow joint angle was the best predictor, explaining 32.6–44.7% of the variance. In both conditions, forearm length followed elbow posture as the next best predictor of elbow load arm length, explaining

18.2–24.4% of the load arm length variance. Together, forearm length and elbow angle explained more than 50% of the variance in elbow load arm lengths on both substrates.

On the ground, forearm length was unassociated with elbow posture and only weakly associated with forelimb posture. Therefore, most of the total correlation between forearm length and elbow load arm length was due to the direct effects of forearm length (Table 4). By contrast, because forearm length was relatively strongly associated with elbow posture during locomotion on the pole, forearm length exerted a positive direct effect on elbow load arm length as well as a equally pronounced positive indirect effect because of the tendency of longer-limbed monkeys to use more flexed elbow postures. Overall, the total association between limb length and load arm length was greater at the elbow than at any other joint.

Hip load arm lengths

Together, hind limb length, thigh angle, hind limb angle and hind limb SRF angle explained 98.4–98.8% of the variation in hip load arm lengths across the ontogenetic sample. As predicted (Fig. 1), longer hip load arms were associated with greater hind limb protraction at peak vertical force and a more cranial inclination of the hind limb SRF. Additionally, the predicted relationship between thigh angles and hip load arms was upheld, with more extended thigh positions exerting a negative effect on hip load arm length. Hind limb angles were consistently the best predictors of hip load arm length, explaining approximately 50% of the variation in hip
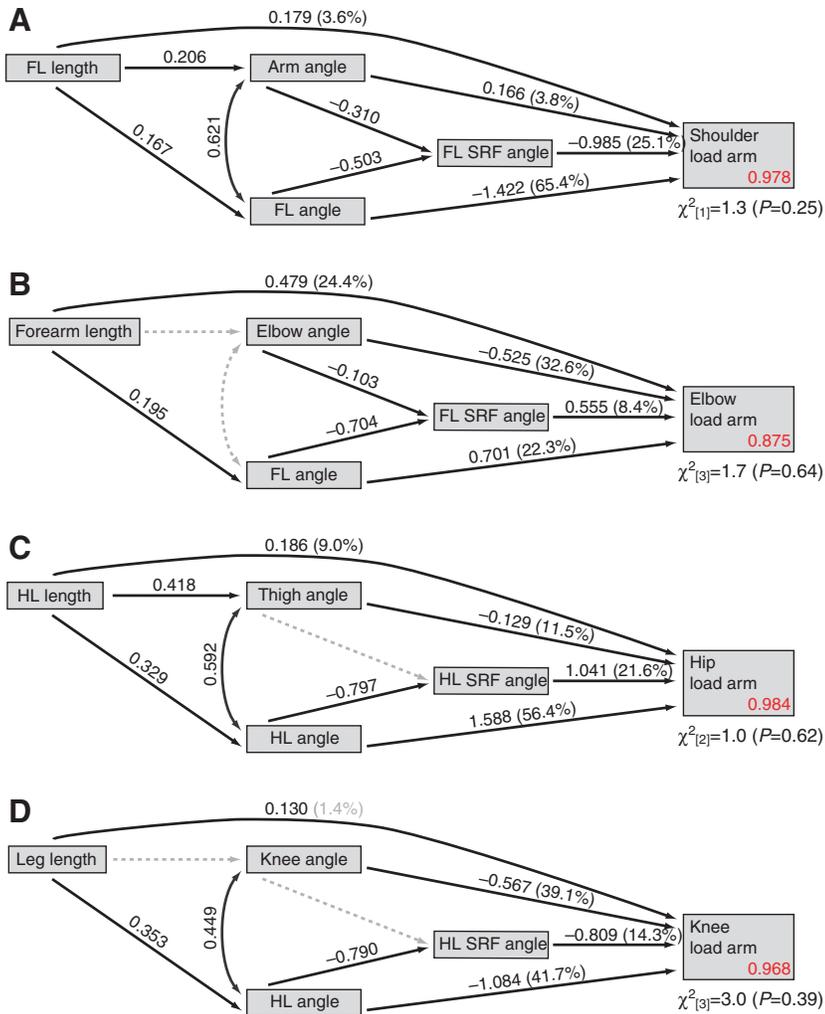
Fig. 5. Path analyses of the influences of limb length, posture and substrate reaction force (SRF) direction on (A) shoulder, (B) elbow, (C) hip and (D) knee joint load arm lengths during locomotion on the ground. Values in parentheses next to the path coefficients are the percentage of load arm length variance uniquely explained by each predictor variable, as determined by hierarchical partitioning. Gray shading indicates that the path or variance partition was not significant. χ^2 tests of model fit are also presented for each joint. The total coefficient of determination (R^2) for each model is also shown in bold red type.

load arm length across substrates. On the ground, hind limb SRF angle was the second best predictor of hip load arm length, explaining 21.6% of the variance. On the pole, the second best predictors were thigh angle and hind limb SRF angle, explaining 28.3% and 23.1% of the variance, respectively.

As predicted, increases in total hind limb length were associated with longer hip joint load arms. However, the explanatory power of hind limb length was generally weak. On the pole, hind limb length was unable to explain a significant portion of load arm variance. Hind limb length performed better on the ground, explaining 9% of the variation in hip load arm length. On the ground, most of the total correlation between hind limb length and hip load arm length was attributable to the indirect influence of limb length on hind limb posture. On the pole, longer-limbed individuals tended to use more extended thigh postures, thus shortening hip load arms, mitigating the slight positive direct effect of hind limb length and reducing the total correlation between hind limb length and hip load arm length (Table 4).

Knee load arm lengths

Leg length, knee angle, hind limb angle and hind limb SRF angle collectively explained 96.8–97.6% of the variance in knee load arm lengths. On the ground, hind limb and knee angles were the best predictors of knee load arm lengths, explaining 41.7% and 39.1% of the variance, respectively. On the pole, hind limb SRF angle was

the best predictor of knee load arm length, explaining 59% of the variance. Knee joint posture was the second best predictor, explaining 20.2% of the variance. As predicted (Fig. 1), increases in knee load arm lengths were associated with greater hind limb retraction, a more caudal orientation of the hind limb SRF and more flexed knee postures.

Leg length was consistently a poor predictor of knee load arm length, explaining just 1.4–4.2% of the variance. On the ground, a negative indirect correlation operating *via* hind limb angle negated the direct effects of leg length on knee joint load arm length, leading to a weak total correlation. Longer-legged individuals tended to use more flexed knee postures on the pole, and most of the total correlation between leg length and knee load arm length could be attributed to this indirect effect operating *via* knee joint posture.

DISCUSSION

Squirrel monkey limb growth during the first 10 months of life was characterized by extremely strong positive allometry, indicating that younger monkeys have relatively short limbs for their size (Fig. 3). All else being equal, relatively short limbs should reduce the distance between joint centers and reaction force vectors, shortening load arms and mitigating joint loading in younger animals. However, hierarchical partitioning and path analyses of the current dataset indicated that variation in anatomical limb length determined only a minor proportion of the variance in load arm lengths at most joints (i.e. less
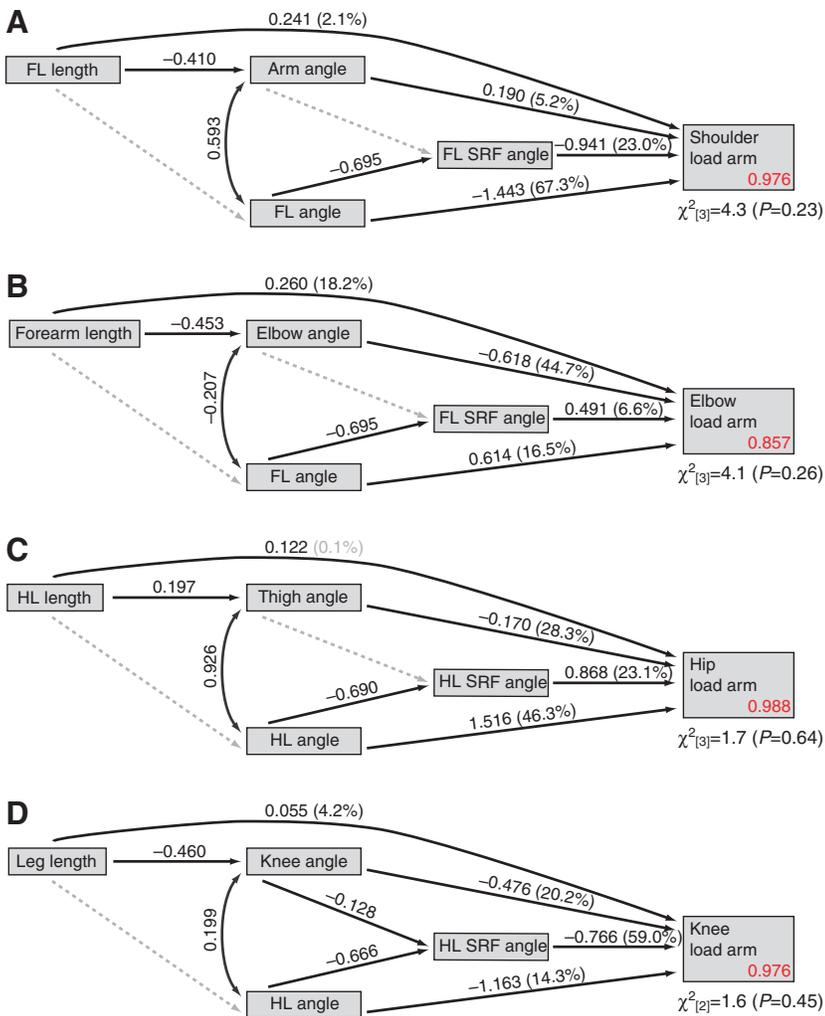
Fig. 6. Path analyses of the influences of limb length, posture, and substrate reaction force (SRF) direction on joint load arm lengths during locomotion on the pole. Data presented as in Fig. 5.

than 10% of the variance at all joints save the elbow; see Figs 5 and 6). Rather, across substrates, load arm lengths primarily varied as a function of posture and SRF angle. Together, joint angle, limb angle and SRF angle accounted for 89.5–97.7% of load arm length variance across all joints except the elbow. The tight correlation between load arm lengths and limb/SRF angles clarifies the predominant lack of ontogenetic variation in most load arm lengths (Table 3), despite significant increases in relative limb length. With the exception of persistent size-related changes in elbow and wrist postures, joint kinematics remained mostly static across the ontogenetic series. Owing to the strut-like behavior of the fore- and hind limbs, SRF angles were strongly associated with limb postures, and therefore ontogenetic variation in SRF orientation was similarly restricted. As a result, size-related changes in relative load arm lengths were primarily restricted to the elbow and, to a lesser extent, the wrist. Only during symmetrical gaits on the ground were ontogenetic changes in limb angles and SRF angles, specifically in the hind limb, sufficient to impact the relative length of load arms during growth.

In contrast to the other joints examined, forearm length alone accounted for 18.2–24.4% of elbow load arm length variance, and forearm length in combination with elbow angle accounted for 57–62.9% of the variance. The relatively strong dependency of elbow load arm length on forearm length is probably the result of two factors: limb geometry and hand posture at peak vertical force. First, the habitually pronated position of the mammalian forearm

during quadrupedal locomotion ensures that the palm, and therefore the estimated hand center of pressure (COP), will be relatively distant from the elbow joint at peak vertical force (Fig. 1E). By contrast, typical hind limb postures ensure that the knee joint and the estimated foot COP could very well be collinear along the axis of the hind limb SRF vector. Second, the metatarsals were held in a significantly more elevated (i.e. digitigrade) position than the metacarpals at peak vertical force (Fig. 7) [$P<0.001$: Watson's two-sample test for circular data (Batschelet, 1981)], further increasing the distance between the estimated hand COP and the elbow joint. Altogether, the increased distance between the estimated hand COP and the elbow permitted more variation in limb length and elbow posture to be translated into load arm length. As such, ontogenetic increases in relative forearm length (Fig. 3) and elbow flexion caused significant size-related increases in relative elbow load arm lengths during most substrate-by-gait conditions (Table 3).

Whereas elbow postures became increasingly flexed as size increased ontogenetically, the wrist joint tended to become more extended (although significant increases in flexion were observed for leading limbs during asymmetrical gaits on the ground). As with the elbow joint, forearm pronation and sub-digitigrade postures at peak vertical force probably increased the distance between the forelimb SRF vector and the wrist joint, permitting more of the variation in wrist angle to be translated into load arm length variation. As a result, ontogenetic increases in wrist extension led to significant

Table 4. Direct and indirect correlations between joint load arm lengths and limb length distal to the joint, as implied by the path models in Figs 5 and 6

	Shoulder	Elbow	Hip	Knee
Ground strides				
Sample size	202	202	98	98
Direct correlation	0.179	0.479	0.186	0.130
Indirect correlation	−0.058	0.061	0.195	−0.157
Via joint angle	0.097	–	−0.054	–
Via limb angle	−0.155	0.061	0.249	−0.157
Total correlation	0.121	0.540	0.381	−0.027
Pole strides				
Sample size	313	313	216	216
Direct correlation	0.241	0.260	0.122	0.055
Indirect correlation	−0.078	0.280	−0.033	0.174
Via joint angle	−0.078	0.280	–	0.174
Via limb angle	–	–	−0.033	–
Total correlation	0.163	0.540	0.089	0.229

decreases in relative wrist load arm lengths during asymmetrical gaits on the pole. Additionally, although hand growth was not measured in the current study, negative ontogenetic allometry of hand length during development, as has been observed in numerous other mammalian taxa (see below; Fig. 8), may have contributed to the observed decrease in wrist load arm lengths.

Relative forelimb SRF magnitudes declined as body size increased in almost all substrate and gait conditions. By contrast, relative hind limb SRF magnitudes tended to increase with body size, although this trend was only significant in half of the substrate-by-gait conditions. Ontogenetic shifts in forelimb–hind limb peak force distribution were associated with a significant caudal translation in whole-body COM position (Young, 2008), a growth-related phenomenon has also been observed in other primates (Turnquist and Wells, 1994; Crompton et al., 1996; Shapiro and Raichlen, 2007).

Ontogenetic shifts in posture and limb force distribution led to several significant size-related increases in relative moments at the elbow, hip and ankle joints. Because relative forelimb SRF magnitudes largely *declined* over development, increases in relative elbow moments were necessarily due to increases in relative load arm lengths alone. By contrast, relative hip and ankle load arm lengths increased significantly only during symmetrical gaits on the ground, although non-significant increasing trends were observed

in most other conditions. Increases in relative hip and ankle moments must therefore be primarily due to relative increases in hind limb SRF magnitudes. Additional ontogenetic changes in joint moments included a relative increase in knee joint moments for trailing limbs during locomotion on the ground and a relative decrease in wrist moments for trailing limbs during asymmetrical gaits on the pole.

Despite well-established differences in the mechanics of symmetrical and asymmetrical gaits (Cavagna et al., 1977; Biewener, 2003), size-related changes in joint mechanics were relatively consistent across gait types within substrates (Table 3). By contrast, across variation in gait type, size-related changes in joint kinematics were consistently observed, more frequently during pole locomotion than during ground locomotion (Table 3). Greater size-related adjustments during pole locomotion probably reflect the stability constraints of moving on narrow, fixed-diameter supports, particularly as body size increases (Cartmill, 1985; Schmitt, 1994; Schmitt, 1998; Schmitt, 1999; Franz et al., 2005; Wallace and Demes, 2008; Young, 2009).

Functional implications for mammalian limb growth and locomotor development

The data presented here demonstrate that a combination of relatively short limbs, more extended elbow postures and changes in limb force distribution allowed infant squirrel monkeys to frequently reduce elbow, hip and ankle joint loading relative to older and larger individuals, even when traveling at the same absolute speed. Such changes should reduce the muscle force needed to maintain posture or effect movement at a joint, although data on the ontogenetic scaling of muscle moment arms in squirrel monkeys would be required to fully corroborate this prediction (i.e. Carrier, 1983; Young, 2005). In the following sections there is a review of what is currently known about the ontogenetic scaling of limb length, joint posture and SRF in other mammalian taxa in order to place the results presented here in a broader comparative context.

Data on ontogenetic allometry of limb growth in primates and other mammalian taxa were collated from the literature and are presented in Fig. 8. These data suggest that positive allometry of limb growth is typical of most mammals. Among primates, long bones grow with positive allometry in almost every species yet studied. Primates showing consistent isometry or negative allometry are either adapted for vertical clinging and leaping (i.e. sifakas, *Propithecus* spp.), a very peculiar form of arboreal locomotion that requires young individuals to be relatively long-limbed in order to
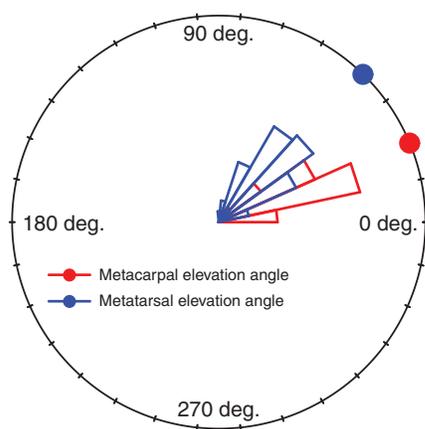

Fig. 7. Angular frequency histograms (Batschelet, 1981) of metacarpal and metatarsal elevation angles relative to the horizontal axis. Filled circles on the perimeter of the plot indicate mean elevation angles.
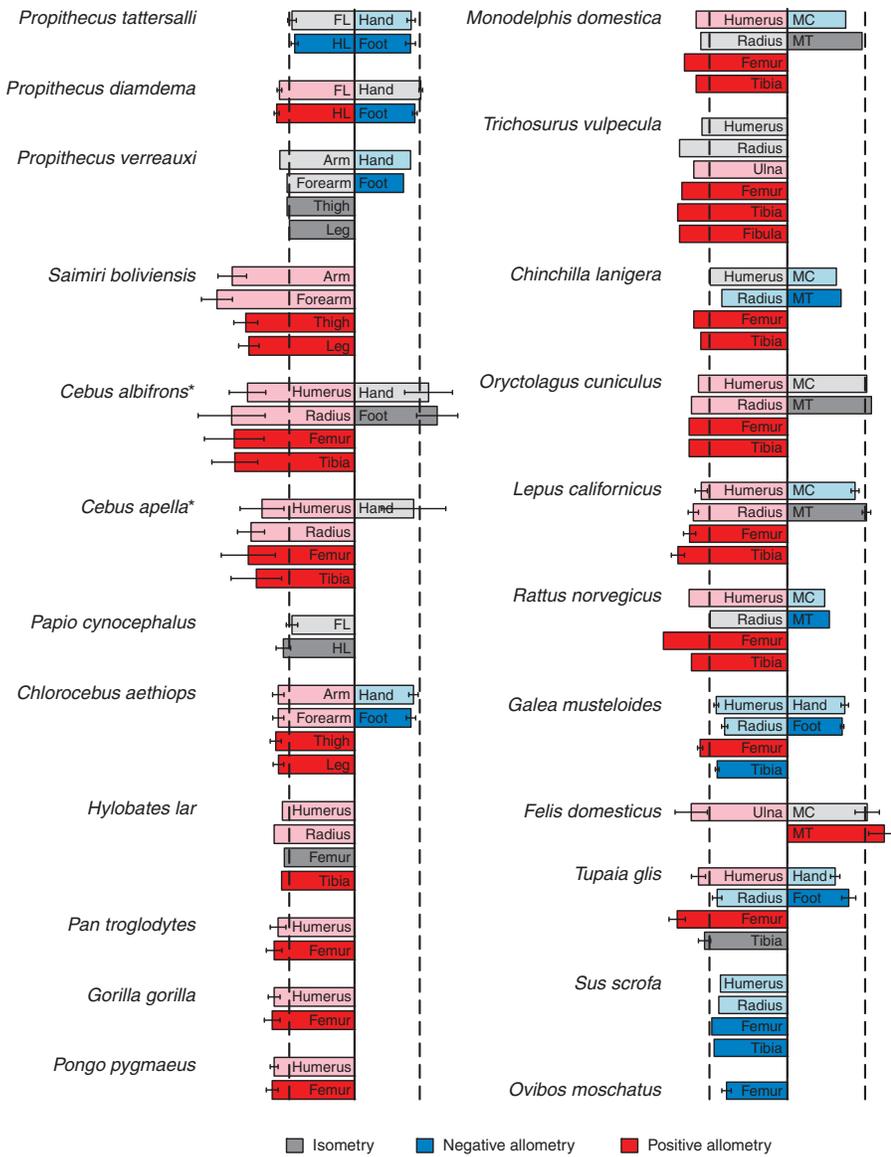
Fig. 8. Scaling of limb growth in primates and other mammalian taxa. In each set of bar graphs, the left hand panels represent complete limbs or stylopodia/zeugopodia (i.e. arms, forearms, thighs or legs) and right-hand panels represent autopodia (metacarpals/metatarsals or complete hands and feet). Forelimb segments are distinguished by lighter shading. Except where indicated by the asterisks next to the species name, allometric exponents were calculated from reduced major axis regressions of segment length on body mass. 95% confidence intervals on the exponents are shown where available. Dashed lines indicate isometry (i.e. slope equal to 0.333). Data sources: *Propithecus tattersalli* [golden-crowned sifaka (Ravosa et al., 1993)] *Propithecus diadema* [diademed sifaka (Ravosa et al., 1993)]; *Propithecus verreauxi* [Verreaux's sifaka (Lawler, 2006)]; *Saimiri boliviensis* [Bolivian squirrel monkey (this study)]; *Cebus albifrons* [white-fronted capuchin monkey (Jungers and Fleagle, 1980)]; *Cebus apella* [tufted capuchin monkey (Jungers and Fleagle, 1980)]; *Papio cynocephalus* [yellow baboon (Raichlen, 2005)]; *Chlorocebus aethiops* [vervet monkey (Turner et al., 1997)]; *Hylobates lar* [white-handed gibbon (Jungers and Cole, 1992)]; *Pan troglodytes* [common chimpanzee (Hartwig-Scherer and Martin, 1992)]; *Gorilla gorilla* [gorilla (Hartwig-Scherer and Martin, 1992)]; *Pongo pygmaeus* [orangutan (Hartwig-Scherer and Martin, 1992)]; *Monodelphis domestica* [gray short-tailed opossum (Lammers and German, 2002)]; *Trichosurus vulpecula* [brushtail possum (Lentle et al., 2006)]; *Chinchilla lanigera* [chinchilla (Lammers and German, 2002)]; *Oryctolagus cuniculus* [domestic white rabbit (Lammers and German, 2002)]; *Lepus californicus* [black-tailed jackrabbit (Carrier, 1983)]; *Rattus norvegicus* [rat (Lammers and German, 2002)]; *Galea musteloides* [cui (Schilling and Petrovitch, 2006)]; *Felis domesticus* [domestic cat (Carrier, 1983)]; *Tupaia glis* [tree shrew (Schilling and Petrovitch, 2006)]; *Sus scrofa* [domestic pig (Liu et al., 1999)]; *Ovibos moschatus* [musk ox (Heinrich et al., 1999)].

produce the necessary accelerations (Ravosa et al., 1993; Demes et al., 1999), or are more terrestrial than most other primates (i.e. baboons, *Papio cynocephalus*). Among other mammalian orders, the only species showing consistent negative allometry of long bone growth are highly precocial and are required to stand and locomote with adults soon after birth (i.e. cuis, *Galea musteloides*, and domestic pigs, *Sus scrofa*). In these species, relatively longer limbs allow perinatal animals to keep pace with older and larger conspecifics during travel and effectively evade predation (Howell, 1944; Pennycuick, 1975; Trillmich et al., 2003).

Whereas the proximal and middle limb segments typically grow with positive allometry, autopodia (i.e. hands and feet) scale to body size with negative allometry or isometry in almost all mammals yet studied. Negative allometry of hand and foot size has been interpreted as an adaptation allowing young primates to cling to their mothers and young quadrupeds in general to negotiate 'adult-sized' substrates and maintain a larger, more secure base of support (Jungers and Fleagle, 1980; Raichlen, 2005; Lawler, 2006). There may, however, be a cost associated with relatively larger hands and feet – by lengthening the load arm of the SRF, relatively longer autopodia may increase joint moments at the wrist and ankle,

particularly if these segments are positioned roughly perpendicular to the SRF vector, as in palmigrade or sub-digitigrade animals. As such, mechanical compensation for ontogenetic limits on force production might be particularly necessary at the wrist and ankle. In fact, strong negative allometry of triceps surae anatomical mechanical advantage at the ankle has previously been documented among black-tailed jackrabbits (Carrier, 1983; Carrier, 1995). Although I was unable to measure hand and foot lengths in the current study, future research should combine allometric analysis of growth in these segments with data on ontogenetic changes in wrist and ankle postures.

Previous studies of postural development in mammals have indicated some variability between taxa, in contrast to the relative uniformity observed in patterns of limb growth across mammals. In most species yet studied, including vervet monkeys, domestic cats, tree shrews and humans, early locomotor efforts are characterized by increased joint flexion (Peters, 1983; Vilensky and Gankiewicz, 1989; Howland et al., 1995; Schilling, 2005; Hallemans et al., 2006). Increased flexion during early locomotion has also been qualitatively noted in tufted capuchin monkeys, rhesus macaques, Japanese macaques, and chimpanzees (Hildebrand, 1967; Kimura, 1987;

Fragaszy, 1990; Nakano, 1996). By contrast, young rats have been shown to use more extended limb postures than older individuals and adults (Westerga and Gramsbergen, 1990). Finally, cuis and baboons show a combination of patterns: increasing flexion at some joints and extension at others (Schilling, 2005; Zeininger, 2007).

Patterns of ontogenetic change in SRF magnitudes are characterized by similar amounts of variability. Kimura (Kimura, 1987; Kimura, 2000) found that relative forelimb and hind peak vertical SRF magnitudes were significantly greater among infant Japanese macaques and chimpanzees than among juveniles and adults. Studies of human locomotor development have also documented patterns of decreasing relative peak vertical SRF magnitudes with increasing age (Beck et al., 1981; Diop et al., 2005). Similarly, using an approximation of SRF based on average limb contact time, Pennycuick (Pennycuick, 1975) estimated that free-ranging infant gnus (*Connochaetes taurinus*) experience significantly greater peak forces than adults traveling at identical absolute speeds. By contrast, other studies of a small, but diverse group of animals have documented isometric variation in SRF magnitudes during ontogeny. Main and Biewener (Main and Biewener, 2004; Main and Biewener, 2007) found that SRF magnitudes scaled in direct proportion to body mass when growing goats (*Capra hircus*) and emus (*Dromaius novaehollandiae*) were traveling at constant relative (i.e. dynamically similar) speeds. Hallemans et al. (Hallemans et al., 2006) also found that after controlling for relative speed, size-adjusted peak vertical and propulsive forces did not change with walking experience (i.e. age) among newly walking humans. As indicated by the level of variation between species and between different studies of the same species (i.e. humans), greater research on the patterns and causes of ontogenetic variation in SRF magnitudes is clearly needed. Additionally, in order to address both the ecological and physiological implications of ontogenetic changes in limb loading, future studies should make comparisons at matched absolute speeds as well as matched relative speeds.

In summary, long bone growth is positively allometric in most mammals, indicating that young mammals are relatively short-limbed for their size. However, it should be noted that the available growth data are strongly biased towards primates, indicating the need for additional ontogenetic study of other mammalian taxa. Patterns of postural development are more variable. Most animals thus far studied, are characterized by increased flexion during early locomotor efforts, although others taxa increased extension or a combination of increased flexion and extension, depending on the joint being examined. Patterns of ontogenetic change in SRF magnitudes appear equally variable, with some studies demonstrating relatively greater limb loading in younger animals whereas others document isometry of force magnitudes.

Pervasive positive allometry of proximal and middle limb segment growth may, by itself, constitute an independent solution to ontogenetic limits on locomotor performance. As illustrated in the current study (Figs 5 and 6) and in previous studies comparing the effects of intra- and interspecific variation in limb length on patterns of joint loading (Polk, 2002; Gruss, 2007), relatively shorter limbs have the potential to shorten joint load arms, thereby mitigating joint moments. The assumption that limb growth determines ontogenetic variation in joint loading motivated Carrier's (Carrier, 1983) and Young's (Young, 2005) morphometric analyses of developmental joint mechanics. However, as reviewed above, the data presented here failed to show a strong direct link between limb length and joint loading in growing squirrel monkeys, despite strong positive allometry

of limb growth. Rather, variation in joint and limb posture were consistently the strongest predictors of variation in joint load arm lengths. It is probable that the flexed joint postures that appear to be typical of most animals during early locomotion are sufficient to lengthen joint load arms, although the precise interaction between developmental changes in posture and limb growth should be evaluated on a species by species basis. Provided SRF magnitudes scale isometrically or with negative allometry, as appears to be the case in the few animals studied thus far, joint moments are likely to be greater as well in animals characterized by increased flexion at early ages. As such, the available data generally support Carrier's (Carrier, 1983) and Young's (Young, 2005) assertion that compensatory growth patterns, such as negative ontogenetic allometry of bony muscle levers, would be required for young mammals to overcome ontogenetic limits on performance, particularly if relative whole-body muscle mass, and available muscle force, were also reduced at early ages.

Why, then, do young squirrel monkeys differ from most other animals in using more extended or similar joint postures relative to older and larger individuals? Among the taxa reviewed above, animals showing increased joint extension early in life are also relatively precocial in their locomotor behavior. Cuis must locomote independently soon after birth (Schilling, 2005). Although rats are born in an altricial state, mature gait patterns are evident at only 20 days after birth (Westerga and Gramsbergen, 1990). Ectothermic vertebrates required to move independently at early ages, such as desert iguanas (*Dipsosaurus dorsalis*), also show greater joint extension as juveniles (Irschick and Jayne, 2000). Path analyses and hierarchical partitioning of the current dataset emphatically demonstrated that walking with erect, strut-like limbs – where the SRF vector is aligned with the limb's axis – was the most effective way of shortening SRF load arms among developing squirrel monkeys. Postural adjustments to SRF load arm lengths have also been cited as the primary means of mitigating limb muscle force requirements between gaits within individuals (Biewener et al., 2004), between differently sized individuals within the same species (Polk, 2002; Gruss, 2007), and between differently sized species (Biewener, 1983; Biewener, 1989) [but see Day and Jayne (Day and Jayne, 2007)]. In sum, extended joints may constitute an effective behavioral means for relatively precocial infants to shorten joint load arms, reduce joint loading, and limit the muscle force required to maintain joint postures. To address the generality of this hypothesis, future studies should include animals encompassing a diverse array of life history strategies, sample a wider, more continuous range of ages (i.e. not just young infants and adults) and combine the performance-related measures examined here with morphometric and experimental data on the ontogenetic scaling of available muscle force and muscle moments arms. Additionally, in order to fully incorporate ontogenetic studies of joint mechanics into an adaptive evolutionary framework (e.g. Arnold, 1983), future research should combine morphometric and lab-based data on musculoskeletal growth and locomotor performance with field-based assessments of survivorship.

Conclusions

This study sought to answer two primary questions. First, among growing squirrel monkeys, how do limb lengths, joint postures, SRF magnitudes, SRF angles, joint load arm lengths and joint moments vary ontogenetically? Second, what proportion of the ontogenetic variation in load arm length can be attributed to limb growth? Previous morphometric studies of mammalian developmental joint

mechanics have assumed that joint postures and SRF scale isometrically during growth and that load arm length is proportional to distal limb length (e.g. Carrier, 1983; Carrier, 1996; Young, 2005). Isometry of joint loading across development would imply that infants, with reduced muscle mass and less available muscle force, would require compensatory musculoskeletal adaptations, such as negative allometry of anatomical mechanical advantage, if they were to match adult-like levels of locomotor performance (Pennycuick, 1975; Carrier, 1983; Carrier, 1996; Trillmich et al., 2003; Main and Biewener, 2004; Young, 2005; Herrel and Gibb, 2006; Lawler, 2006). Contrary to predictions, joint postures, SRF vectors, joint load arm lengths and joint moments frequently did not scale isometrically to body size in growing squirrel monkeys. Rather, ontogenetic changes in joint postures and body mass distribution mitigated joint loading at the elbow, hip and ankle during several of the substrate-by-gait conditions examined here. A full assessment of the realized benefits of such ontogenetic changes in joint loading requires further data on the scaling of muscle force and muscle moment arms during growth.

In summary, the size-related kinematic and kinetic changes documented in this study constitute an example of 'behavioral' compensation for ontogenetic limits on locomotor performance, a phenomenon previously identified only in ectothermic vertebrates (Jayne and Bennett, 1990; Irschick, 2000; Miles, 2004; Irschick et al., 2005; Dial et al., 2008), suggesting that growing mammals may use a combination of anatomical and behavioral means to overcome ontogenetic limits on locomotor performance. The existence of such behavioral mechanisms may challenge the status of allometric musculoskeletal growth trajectories as 'necessary' mammalian solutions to ontogenetic limits on locomotor performance (cf. Carrier, 1983), at least among species characterized by patterns of locomotor development similar to the squirrel monkeys observed here. Morphological adaptations to ontogenetic limits on locomotion, such as negative ontogenetic allometry of anatomical mechanical advantage, may be more critical among animals characterized by more flexed limb postures early in life or in species where young are under extreme selective pressure to accelerate quickly to evade predation, such as the jackrabbits studied by Carrier (Carrier, 1983).

LIST OF ABBREVIATIONS

SRF	substrate reaction force
r	average muscle moment arm length (weighted by individual muscle force)
R	SRF load arm length
$\mathbf{F}_S$	SRF magnitude
$\mathbf{F}_M$	total muscle force
$\mathbf{F}_{x(Vpk)}$	magnitude of the fore–aft component of the SRF at peak vertical force
$\mathbf{F}_{y(Vpk)}$	magnitude of the vertical component of the SRF at peak vertical force
M_b	body mass

REFERENCES

Arnold, S. J. (1983). Morphology, performance and fitness. *Am. Zool.* **23**, 347-361.

Atzeva, M., Demes, B., Kirkbride, M. L., Burrows, A. M. and Smith, T. D. (2007). Comparison of hind limb muscle mass in neonate and adult prosimian primates. *J. Hum. Evol.* **52**, 231-242.

Barclay, O. R. (1953). Some aspects of the mechanics of mammalian locomotion. *J. Exp. Biol.* **30**, 116-120.

Batschelet, E. (1981). *Circular Statistics in Biology*. New York: Academic Press.

Beck, R. J., Andriacchi, T. P., Kuo, K. N., Fermier, R. W. and Galante, J. O. (1981). Changes in the gait patterns of growing children. *J. Bone Joint Surg. Am.* **63**, 1452-1457.

Biewener, A. A. (1983). Allometry of quadrupedal locomotion: the scaling of duty factor, bone curvature and limb orientation to body size. *J. Exp. Biol.* **105**, 147-171.

Biewener, A. A. (1989). Scaling body support in mammals: limb posture and muscle mechanics. *Science* **245**, 45-48.

Biewener, A. A. (2003). *Animal Locomotion*. Oxford: Oxford University Press.

Biewener, A. A. and Full, R. J. (1992). Force platform and kinematic analysis. In *Biomechanics: Structures and Systems* (ed. A. A. Biewener), pp. 45-73. Oxford: Oxford University Press.

Biewener, A. A., Farley, C. T., Roberts, T. J. and Temaner, M. (2004). Muscle mechanical advantage of human walking and running: implications for energy cost. *J. Appl. Physiol.* **97**, 2266-2274.

Boinski, S. (1987). Birth synchrony in squirrel monkeys (*Saimiri oerstedi*): a strategy to reduce neonatal predation. *Behav. Ecol. Sociobiol.* **21**, 393-400.

Boinski, S. (1989). The positional behavior and substrate use of squirrel monkeys: ecological implications. *J. Hum. Evol.* **18**, 659-677.

Boinski, S. (1999). The social organization of squirrel monkeys: implications for ecological models of social evolution. *Evol. Anthropol.* **8**, 101-112.

Boinski, S. and Fragaszy, D. M. (1989). The ontogeny of foraging in squirrel monkeys, *Saimiri oerstedi. Anim. Behav.* **37**, 415-428.

Boinski, S., Sughrue, K., Selvaggi, L., Quatrone, R., Henry, M. and Cropp, S. (2002). An expanded test of the ecological model of primate social evolution: competitive regimes and female bonding in three species of squirrel monkeys (*Saimiri oerstedii, S. boliviensis,* and *S. sciureus*). *Behaviour* **139**, 227-261.

Boinski, S., Kauffman, L., Westoll, A., Stickler, C. M., Cropp, S. and Ehmke, E. (2003). Are vigilance, risk from avian predators and group size consequences of habitat structure? A comparison of three species of squirrel monkey (*Saimiri oerstedii, S. boliviensis*, and *S. sciureus*). *Behaviour* **140**, 1421-1467.

Bolter, D. and Zihlman, A. (2007). Primate growth and development: a functional and evolutionary perspective. In *Primates in Perspective* (ed. C. J. Campbell, A. Fuentes, K. C. MacKinnon, M. A. Panger and S. K. Bearder), pp. 408-422. New York: Oxford University Press.

Carrier, D. R. (1983). Postnatal ontogeny of the musculo-skeletal system in the Black-tailed jack rabbit (*Lepus californicus*). *J. Zool. Lond.* **201**, 27-55.

Carrier, D. R. (1995). Ontogeny of jumping performance in the black-tailed jackrabbit (*Lepus californicus*). *Zool. Anal. Complex Sy.* **98**, 309-313.

Carrier, D. R. (1996). Ontogenetic limits on locomotor performance. *Physiol. Zool.* **69**, 467-488.

Carrier, D. R. and Leon, L. R. (1990). Skeletal growth and function in the California gull (*Larus californicus*). *J. Zool. Lond.* **222**, 375-389.

Cartmill, M. (1985). Climbing. In *Functional Vertebrate Morphology* (ed. M. Hildebrand, D. M. Bramble, K. F. Liem and D. B. Wake), pp. 73-88. Cambridge, MA: Harvard University Press.

Cavagna, G. A., Heglund, N. C. and Taylor, C. R. (1977). Mechanical work in terrestrial locomotion: two basic mechanisms for minimizing energy expenditure. *Am. J. Physiol.* **233**, R243-R261.

Chevan, A. and Sutherland, M. (1991). Hierarchical partitioning. *Am. Stat.* **45**, 90-96.

Crompton, R. H., Li, Y., Alexander, R. M., Wang, W. and Günther, M. M. (1996). Segment inertial properties of primates: new techniques for laboratory and field studies of locomotion. *Am. J. Phys. Anthropol.* **99**, 547-570.

Day, L. M. and Jayne, B. C. (2007). Interspecific scaling of the morphology and posture of the limbs during the locomotion of cats (Felidae). *J. Exp. Biol.* **210**, 642-654.

Demes, B., Fleagle, J. G. and Jungers, W. L. (1999). Takeoff and landing forces of leaping strepsirhine primates. *J. Hum. Evol.* **37**, 279-292.

Dial, K. P., Greene, E. and Irschick, D. J. (2008). Allometry of behavior. *Trends Ecol. Evol.* **23**, 394-401.

Diop, M., Rahmani, A., Belli, A., Gautheron, V., Geyssant, A. and Cottalorda, J. (2005). Influence of speed variation and age on ground reaction forces and stride parameters of children's normal gait. *Int. J. Sports Med.* **26**, 682-687.

Elias, M. F. (1977). Relative maturing of cebus and squirrel monkeys at birth and during infancy. *Dev. Psychobiol.* **10**, 519-528.

Falster, D. S., Warton, D. I. and Wright, I. J. (2003). (S)MATR: Standardised major axis tests and routines. *Version 1.0. http://www.bio.mq.edu.au/ecology/SMATR*.

Fedigan, L. M., Rosenberger, A. L., Boinski, S., Norconk, M. A. and Garber, P. A. (1996). Critical issues in Cebine evolution and behavior. In *Adaptive Radiations of Neotropical Primates* (ed. M. A. Norconk, A. L. Rosenberger and P. A. Garber), pp. 219-228. New York: Plenum Press.

Fontaine, R. (1990). Positional behavior in *Saimiri boliviensis* and *Ateles geoffroyi*. *Am. J. Phys. Anthropol.* **82**, 485-508.

Fragaszy, D. M. (1990). Early behavioral development in capuchins (*Cebus*). *Folia Primatol. (Basel)* **54**, 119-128.

Fragaszy, D. M., Baer, J. and Adams-Curtis, L. (1991). Behavioral development and maternal care in tufted capuchins (*Cebus apella*) and squirrel monkeys (*Saimiri sciureus*) from birth through seven months. *Dev. Psychobiol.* **24**, 375-393.

Franz, T. M., Demes, B. and Carlson, K. J. (2005). Gait mechanics of lemurid primates on terrestrial and arboreal substrates. *J. Hum. Evol.* **48**, 199-217.

Garber, P. A. and Leigh, S. R. (1997). Ontogenetic variation in small-bodied New World primates: implications for patterns of reproduction and infant care. *Folia Primatol. (Basel)* **68**, 1-22.

Goldspink, D. F. (1980). Physiological factors influencing protein turnover and muscle growth in mammals. In *Development and Specialization of Skeletal Muscle* (ed. D. F. Goldspink). Cambridge: Cambridge University Press.

Grand, T. I. (1977). Body weight: its relation to tissue composition, segment distribution, and motor function. II. Development of *Macaca mulatta. Am. J. Phys. Anthropol.* **47**, 241-248.

Grand, T. I. (1983). The anatomy of growth and its relation to locomotor capacity in *Macaca*. In *Advances in the Study of Mammalian Behavior*, vol. 7 (ed. J. F. Eisenberg and D. G. Kleiman), pp. 5-23. Shippensburg, PA: American Society of Mammalogists.

Gray, J. (1968). *Animal Locomotion.* New York: Norton.

Gruss, L. T. (2007). Limb length and locomotor biomechanics in the genus *Homo*: an experimental study. *Am. J. Phys. Anthropol.* **134**, 106-116.

Hallemans, A., De Clercq, D. and Aerts, P. (2006). Changes in 3D joint dynamics during the first 5 months after the onset of independent walking: a longitudinal follow-up study. *Gait Posture* **24**, 270-279.

Hartwig, W. C. (1995). Effect of life history on the squirrel monkey (Platyrrhini: *Saimiri*) cranium. *Am. J. Phys. Anthropol.* **97**, 435-449.

Hartwig-Scherer, S. and Martin, R. D. (1992). Allometry and prediction in hominoids: a solution to the problem of intervening variables. *Am. J. Phys. Anthropol.* **88**, 37-57.

Hedrick, T. (2007). "DLT Data Viewer 2", Digitizing and DLT in MATLAB. *http://www.unc.edu/~thedrick/software1.html.*

Heglund, N. C. (1981). A simple design for a force-plate to measure ground reaction forces. *J. Exp. Biol.* **93**, 333-338.

Heinrich, R. E., Ruff, C. B. and Adamczewski, J. Z. (1999). Ontogenetic changes in mineralization and bone geometry in the femur of muskoxen (*Ovibos moschatus*). *J. Zool. Lond.* **247**, 215-223.

Herrel, A. and Gibb, A. C. (2006). Ontogeny of performance in vertebrates. *Physiol. Biochem. Zool.* **79**, 1-6.

Hildebrand, M. (1967). Symmetrical gaits of primates. *Am. J. Phys. Anthropol.* **26**, 119-130.

Hildebrand, M. (1976). Analysis of tetrapod gaits: general considerations and symmetrical gaits. In *Neural Control of Locomotion* (ed. R. M. Herman, S. Grillner, P. S. G. Stein and D. G. Stuart), pp. 203-236. New York: Plenum Press.

Howell, A. B. (1944). *Speed in Animals.* New York: Hafner Publishing Company.

Howland, D. R., Bregman, B. S. and Goldberger, M. E. (1995). The development of quadrupedal locomotion in the kitten. *Exp. Neurol.* **135**, 93-107.

Huxley, J. W. (1932). *Problems in Relative Growth.* Cambridge: Cambridge University Press.

Irschick, D. J. (2000). Effects of behaviour and ontogeny on the locomotor performance of a West Indian lizard, *Anolis lineatopus. Funct. Ecol.* **14**, 438-444.

Irschick, D. J. and Jayne, B. C. (2000). Size matters: ontogenetic variation in the three-dimensional kinematics of steady-speed locomotion in the lizard *Dipsosaurus dorsalis. J. Exp. Biol.* **203**, 2133-2148.

Irschick, D. J., Herrel, A. V., Vanhooydonck, B., Huyghe, K. and Van Damme, R. (2005). Locomotor compensation creates a mismatch between laboratory and field estimates of escape speed in lizards: a cautionary tale for performance-to-fitness studies. *Evolution* **59**, 1579-1587.

Jayne, B. C. and Bennett, A. F. (1990). Selection on locomotor performance capacity in a natural population of garter snakes. *Evolution* **44**, 1204-1229.

Johnson, V. S. (1998). *A Comparative Study of the Skeletal and Muscular Development of the Squirrel Monkey and How it Relates to the Locomotor Patterns Between the Infant and the Adult (Saimiri boliviensis)*. M.Sc. Thesis, University of Arizona: Tucson, AZ, USA.

Jungers, W. L. and Cole, M. S. (1992). Relative growth and shape of the locomotor skeleton in lesser apes. *J. Hum. Evol.* **23**, 93-105.

Jungers, W. L. and Fleagle, J. G. (1980). Postnatal growth allometry of the extremities in *Cebus albifrons* and *Cebus apella*: a longitudinal and comparative study. *Am. J. Phys. Anthropol.* **53**, 471-478.

Kaack, B., Walker, L. and Brizzee, K. R. (1979). The growth and development of the squirrel monkey (*Saimiri sciureus*). *Growth* **43**, 116-135.

Kimura, T. (1987). Development of chimpanzee locomotion on level surfaces. *Hum. Evol.* **2**, 107-119.

Kimura, T. (2000). Development of quadrupedal locomotion on level surfaces in Japanese macaques. *Folia Primatol. (Basel)* **71**, 323-333.

Lammers, A. R. and German, R. Z. (2002). Ontogenetic allometry in the locomotor skeleton of specialized half-bounding mammals. *J. Zool. Lond.* **258**, 485-495.

Lawler, R. R. (2006). Sifaka positional behavior: ontogenetic and quantitative genetic approaches. *Am. J. Phys. Anthropol.* **131**, 261-271.

Lentle, R. G., Kruger, M. C., Mellor, D. J., Birtles, M. and Moughan, P. J. (2006). Limb development in pouch young of the brushtail possum (*Trichosurus vulpecula*) and tammar wallaby (*Macropus eugenii*). *J. Zool.* **270**, 122-131.

Li, C. C. (1975). *Path Analysis: A Primer.* Pacific Grove, CA: The Boxwood Press.

Liu, M. F., He, P., Aherne, F. X. and Berg, R. T. (1999). Postnatal limb bone growth in relation to live weight in pigs from birth to 84 days of age. *J. Anim. Sci.* **77**, 1693-1701.

MacNally, R. (2002). Multiple regression and inference in ecology and conservation biology: further comments on identifying important predictor variables. *Biodivers. Conserv.* **11**, 1397-1401.

MacNally, R. and Walsh, C. J. (2004). Hierarchical partitioning public-domain software. *Biodivers. Conserv.* **13**, 659-660.

Main, R. P. and Biewener, A. A. (2004). Ontogenetic patterns of limb loading, *in vivo* bone strains and growth in the goat radius. *J. Exp. Biol.* **207**, 2577-2588.

Main, R. P. and Biewener, A. A. (2007). Skeletal strain patterns and growth in the emu hindlimb during ontogeny. *J. Exp. Biol.* **210**, 2676-2690.

Miles, D. B. (2004). The race goes to the swift: fitness consequences of variation in sprint performance in juvenile lizards. *Evol. Ecol. Res.* **6**, 63-75.

Mitchell, C. L. (1990). *The Ecological Basis for Female Social Dominance: A Behavioral Study of the Squirrel Monkey (Saimiri sciureus) in the Wild.* PhD Thesis, Princeton University: Princeton, NJ, USA.

Mosimann, J. E. and James, F. C. (1979). New statistical methods for allometry with application to Florida red-winged blackbirds. *Evolution* **33**, 444-459.

Nakano, Y. (1996). Footfall patterns in the early development of the quadrupedal walking of Japanese macaques. *Folia Primatol. (Basel)* **66**, 113-125.

Ozkaya, N. and Nordin, M. (1999). *Fundamentals of Biomechanics: Equilibrium, Motion and Deformation.* New York: Springer.

Pennycuick, C. J. (1975). On the running of the gnu (*Connochaetes taurinus*) and other animals. *J. Exp. Biol.* **63**, 775-799.

Peters, S. E. (1983). Postnatal development of gait behavior and functional allometry in the domestic cat. *J. Zool. Lond.* **199**, 461-486.

Pitman, E. T. G. (1939). A note on normal correlation. *Biometrika* **31**, 9-12.

Polk, J. D. (2001). *The Influence of Body Size and Proportions on Primate Quadrupedal Locomotion.* Ph.D thesis, Stony Brook University: Stony Brook, NY, USA.

Polk, J. D. (2002). Adaptive and phylogenetic influences on musculoskeletal design in cercopithecine primates. *J. Exp. Biol.* **205**, 3399-3412.

R Development Core Team. (2008). R: A language and environment for statistical computing. Vienna, Austria: R Foundation for Statistical Computing.

Raichlen, D. A. (2005). Ontogeny of limb mass distribution in infant baboons (*Papio cynocephalus*). *J. Hum. Evol.* **49**, 452-467.

Raichlen, D. A. (2006). Effects of limb mass distribution on mechanical power outputs during quadrupedalism. *J. Exp. Biol.* **209**, 633-644.

Ravosa, M. J., Meyers, D. M. and Glander, K. E. (1993). Relative growth of the limbs and trunk in sifakas-heterochronic, ecological, and functional considerations. *Am. J. Phys. Anthropol.* **92**, 499-520.

Ricker, W. E. (1984). Computation and uses of central trend lines. *Can. J. Zool.* **62**, 1897-1905.

Riskin, D. K., Bertram, J. E. A. and Hermanson, J. W. (2005). Testing the hindlimb-strength hypothesis: non-aerial locomotion by Chiroptera is not constrained by the dimensions of the femur or tibia. *J. Exp. Biol.* **208**, 1309-1319.

Schermelleh-Engel, K., Moosbrugger, H. and Muller, H. (2003). Evaluating the fit of structural equation models: tests of significance and descriptive goodness of fit measures. *Methods Psychol. Res. Online* **8**, 23-74.

Schilling, N. (2005). Ontogenetic development of locomotion in small mammals – a kinematic study. *J. Exp. Biol.* **208**, 4013-4034.

Schilling, N. and Petrovitch, A. (2006). Postnatal allometry of the skeleton in *Tupaia glis* (Scandentia: Tupaiidae) and *Galea musteloides* (Rodentia: Caviidae): a test of the three-segment limb hypothesis. *Zoology* **109**, 148-162.

Schmitt, D. (1994). Forelimb mechanics as a function of substrate type during quadrupedalism in two anthropoid primates. *J. Hum. Evol.* **26**, 441-457.

Schmitt, D. (1998). Forelimb mechanics during arboreal and terrestrial quadrupedalism in Old World monkeys. In *Primate Locomotion: Recent Advances* (ed. E. Strasser, J. Fleagle, A. Rosenberger and H. McHenry), pp. 175-200. New York, NY: Plenum Press.

Schmitt, D. (1999). Compliant walking in primates. *J. Zool. Lond.* **248**, 149-160.

Shapiro, L. J. and Raichlen, D. A. (2007). Center of mass position, quadrupedalism, and stability: where do primates fall? *Am. J. Phys. Anthropol.* **44**, 215.

Smith, R. J. and Jungers, W. L. (1997). Body mass in comparative primatology. *J. Hum. Evol.* **32**, 523-559.

Sokal, R. R. and Rohlf, F. J. (1995). *Biometry.* New York: W. H. Freeman.

Stone, A. I. (2006). Foraging ontogeny is not linked to delayed maturation in squirrel monkeys (*Saimiri sciureus*). *Ethology* **112**, 105-115.

Terborgh, J. (1983). *Five New World Primates: A Study in Comparative Ecology.* Princeton, NJ: Princeton University Press.

Trillmich, F., Bieneck, M., Geissler, E. and Bischof, H. J. (2003). Ontogeny of running performance in the wild guinea pig (*Cavia aperea*). *Mamm. Biol.* **68**, 214-223.

Turner, T. R., Anapol, F. and Jolly, C. J. (1997). Growth, development, and sexual dimorphism in vervet monkeys (*Cercopithecus aethiops*) at four sites in Kenya. *Am. J. Phys. Anthropol.* **103**, 19-35.

Turnquist, J. E. and Wells, J. P. (1994). Ontogeny of locomotion in rhesus macaques (*Macaca mulatta*): I. Early postnatal ontogeny of the musculoskeletal system. *J. Hum. Evol.* **26**, 487-499.

Vilensky, J. A. and Gankiewicz, E. (1989). Early development of locomotor behavior in vervet monkeys. *Am. J. Primatol.* **17**, 11-25.

Wallace, I. J. and Demes, B. (2008). Symmetrical gaits of *Cebus apella*: implications for the functional significance of diagonal sequence gait in primates. *J. Hum. Evol.* **54**, 783-794.

Werner, E. E. and Gillam, J. F. (1984). The ontogenetic niche and species interactions in size-structured populations. *Annu. Rev. Ecol. Syst.* **15**, 393-425.

Westerga, J. and Gramsbergen, A. (1990). The development of locomotion in the rat. *Dev. Brain Res.* **57**, 163-174.

Winter, D. A. (2005). *Biomechanics and Motor Control of Human Movement.* Hoboken, NJ: John Wiley.

Witte, H., Biltzinger, J., Hackert, R., Schilling, N., Schmidt, M., Reich, C. and Fischer, M. S. (2002). Torque patterns of the limbs of small therian mammals during locomotion on flat ground. *J. Exp. Biol.* **205**, 1339-1353.

Young, J. W. (2005). Ontogeny of muscle mechanical advantage in capuchin monkeys (*Cebus albifrons* and *Cebus apella*). *J. Zool. Lond.* **267**, 351-362.

Young, J. W. (2008). *Ontogeny of Locomotion in* Saimiri boliviensis *and* Callithrix jacchus*: Implications for Primate Locomotor Ecology and Evolution.* Phd Thesis, Stony Brook University: Stony Brook, NY, USA.

Young, J. W. (2009). Substrate determines asymmetrical gait dynamics in marmosets (*Callithrix jacchus*) and squirrel monkeys (*Saimiri boliviensis*). *Am. J. Phys. Anthropol.* **138**, 403-420.

Zeininger, A. D. (2007). *Ontogeny of Digitigrade Hand and Foot Postures in Infant Baboons (Papio cynocephalus).* MA Thesis, University of Texas at Austin: Austin, TX, USA.